Core Ideas

- We tested a range of dual-permeability parameterizations at plot and catchment scale.
- Well-performing parameters at plot scale did not clearly improve catchment simulation.
- Vertical preferential flow was important for simulating plot-scale observations.
- At catchment scale, it appeared more important to consider fast lateral subsurface flow.
- This showed that different nonuniform flow processes are critical at different scales.

B. Glaser and J. Klaus, Catchment and Eco-Hydrology Research Group, Luxembourg Institute of Science and Technology, L-4362 Esch/Alzette, Luxembourg; B. Glaser and L. Hopp, Dep. of Hydrology, Univ. of Bayreuth, 95447 Bayreuth, Germany; C. Jackisch, Chair of Hydrology, Institute of Water Resources and River Basin Management, Karlsruhe Institute of Technology, 76131 Karlsruhe, Germany. C. Jackisch currently at: Dep. of Landscape Ecology and Environmental Systems Analysis, Institute of Geoecology, Technische Universität Braunschweig, Langer Kamp 19c, 38106 Braunschweig, Germany. *Corresponding author (barbara.glaser@list.lu).

How Meaningful are Plot-Scale Observations and Simulations of Preferential Flow for Catchment Models?

Barbara Glaser,* Conrad Jackisch, Luisa Hopp, and Julian Klaus

Despite ubiquitous field observations of nonuniform flow processes, preferential flow paths are rarely considered in hydrological models, especially at catchment scale. In this study, we investigated the extent to which plot-scale observations of preferential flow paths are informative for rainfall–runoff simulations at larger scales. We used data from three plot-scale irrigation experiments in the Weierbach catchment (Luxembourg) to identify preferential flow parameterizations via a Monte Carlo simulation with HydroGeoSphere. Subsequently, we tested whether these parameter sets could be used directly to simulate the hydrological response of the Weierbach headwater with a HydroGeoSphere catchment model. The Monte Carlo simulations showed that the different depth profiles of Br$^-$ tracer observed in irrigation experiments could be reproduced when vertical preferential flow was simulated with a dual-permeability approach. However, it was not possible to identify unique parameter values for preferential flow. The direct transfer of a range of different dual-permeability parameter sets to the catchment model revealed that the variability of simulated hydrometric catchment responses (discharge and soil moisture over 18 mo) was independent of the variability among the three irrigation experiments. More importantly, the dual-permeability approach did not improve the match between simulated and observed discharge and soil moisture responses compared with the single-domain reference model, where multiple soil layers with differing hydraulic conductivities had already been implemented. This suggests that including structures that allow nonuniform lateral flow was more important for reproducing the hydrological response in the Weierbach catchment than the vertical preferential flow observed at plot scale.

Abbreviations: 3D, three-dimensional; MC, Monte Carlo; NSE, Nash–Sutcliffe efficiency.

It is often criticized that the majority of hydrological models neglect or poorly represent preferential flow processes and therefore miss an important feature of subsurface processes (e.g., Beven and Germann, 2013; Weiler, 2017). At the same time, the integrated effect of preferential flow paths on catchment response remains under discussion (Beven and Germann, 2013; Weiler, 2017). To date, many experimental studies at plot (<5 m^2) and hillslope (5 m^2–1 ha) scales have shown that vertical and lateral preferential flow have a crucial impact on the timing and quantity of water flow and solute transport (e.g., Vogel et al., 2006; Rosenbom et al., 2009; Anderson et al., 2009; van Schaik et al., 2010; Klaus et al., 2013, 2014; Laine-Kaulio et al., 2014; Jackisch et al., 2017; Scaini et al., 2017). Yet, direct observations of preferential flow pathways at catchment scale (>1 ha) are rather scarce. Recently, Wilson et al. (2016) observed that networks of large soil pipes can effectively connect the hillslope areas with the catchment outlet via lateral preferential flow. Other work at catchment scale has relied on soil moisture sensor networks (Liu and Lin, 2015; Wiekenkamp et al., 2016) to analyze the spatiotemporal occurrence of preferential flow across two forested catchments (7.9 ha and 38.5 ha, respectively). These two studies demonstrated that the occurrence of vertical preferential flow was highly variable in space across the two catchments investigated. Based on their field results, Liu and Lin (2015) identified a "hidden" preferential flow network in the subsurface. However, such

an experimental setup does not allow the relevance of small-scale variabilities in preferential flow patterns and in local subsurface flow networks to be analyzed for the rainfall–runoff response at the catchment outlet.

Modeling approaches can help to bridge the gap between observations of preferential flow at plot and hillslope scale and the understanding of the effect of preferential flow on integrated catchment responses. However, as is the case for the experimental investigations, there is a discrepancy between the number of simulations that include preferential flow at plot and hillslope scale (e.g., Weiler and McDonnell, 2007; Klaus and Zehe, 2010, 2011; Laine-Kaulio et al., 2014; Frey et al., 2016; Kukemilks et al., 2018a; Reck et al., 2018) and the number of simulations that include preferential flow at catchment scale (e.g., Krzeminska et al., 2013; Steinbrich et al., 2016; Villamizar and Brown, 2017; Kukemilks et al., 2018b). Consequently, the number of modeling studies that have explicitly analyzed the effect of preferential flow on catchment response by comparing simulations with and without preferential flow is limited (Beckers and Alila, 2004; Christiansen et al., 2004; Zhang et al., 2006; van Schaik et al., 2014; Yu et al., 2014; De Schepper et al., 2015). An increased number of such studies could be a valuable asset for the currently limited understanding of the circumstances, processes, and degree to which preferential flow has a relevant effect on integrated catchment response and thus requires explicit parameterization and simulation.

In practical terms, two main challenges hinder preferential flow concepts from being included more often in distributed, physically based catchment-scale simulations: (i) finding a proper mathematical process description that is adequate for the scale, and (ii) finding adequate model parameters for the process description (cf. Beven and Germann, 2013; Jarvis et al., 2016). While numerous plot-scale studies have focused on advancing accurate descriptions of flow and exchange processes within explicitly implemented macropores and fractures (e.g., Vogel et al., 2006; Scheibe et al., 2015; Jackisch and Zehe, 2018), explicit implementations of discrete macropore and fracture geometries for an entire catchment are (currently) not feasible from a computational and parameterization point of view (Jarvis et al., 2016). Instead, the most common representations of preferential flow processes in existing catchment simulations are dual-domain approaches, which separate the subsurface into two interacting matrix and preferential flow domains with differing hydraulic properties (e.g., Kordilla et al., 2012; van Schaik et al., 2014; Wang et al., 2014; Yu et al., 2014; De Schepper et al., 2015; Jarvis et al., 2016; Steinbrich et al., 2016; Villamizar and Brown, 2017). The physical adequacy of the most commonly used equations within the dual-domain approach (e.g., Darcy equation, Richards equation, Green-Ampt infiltration) for catchment scale has been debated (cf. Beven and Germann, 2013; Jarvis et al., 2016). Aside from this fact, the implicit representation of the subsurface structure with two coexisting bulk domains is a strong simplification of the real preferential flow network. Yet, many of the studies that included preferential flow processes for simulating catchment responses have simplified the spatial representation of

the catchment even more, e.g., by proportionally combining the outputs of several representative one-dimensional dual-permeability simulations to a catchment response (Wang et al., 2014; Villamizar and Brown, 2017), performing a two-dimensional dual-permeability simulation for a representative cross-section through the catchment (e.g., Kordilla et al., 2012), or using spatially distributed three-dimensional (3D) dual-permeability simulations with lumped formulations for lateral (Krzeminska et al., 2013) or groundwater flow (van Schaik et al., 2014). The question of which spatial simplifications of preferential flow are necessary and suitable for appropriate catchment-scale simulations with acceptable computational costs remains open.

Regardless of the representation chosen for preferential flow, the identification of an adequate parameterization to simulate preferential flow is challenging (Beven and Germann, 2013). Most existing catchment modeling approaches rely on parameter calibration or a parameterization based on literature values. Only a few studies have parameterized preferential flow (at least partly) based on measurements of study site characteristics such as saturated hydraulic conductivity, water retention curve, crack density, and fracture aperture (e.g., Kordilla et al., 2012; Steinbrich et al., 2016; Loritz et al., 2017; Kukemilks et al., 2018b). The problem of parameter calibration in physically based models is that (i) the optimized parameters may not capture the real physics of the system, (ii) parameters may not uniquely converge due to equifinality, and (iii) calibration may require a large number of model runs, with the latter being mainly restrictive for physically based, distributed, 3D catchment simulations with long computational times. Therefore, the calibration of physically based 3D catchment models including preferential flow barely exists today (exception, Yu et al., 2014). A direct parameterization based on field observations is challenging because measurements can only capture local characteristics of a catchment and it is hardly feasible to perform sufficient measurements to fully assess the heterogeneity within a catchment.

A promising approach for identifying an observation-based parameterization of preferential flow for catchment simulations is to derive parameters in simulations of detailed plot-scale observations and to then use these parameters for informing catchment-scale simulations (e.g., Vogel and Roth, 2003; Beven and Germann, 2013; Cadini et al., 2013). Previous studies have realized such an upscaling of preferential flow simulations from plot to hillslope or catchment scale but have lacked validation of the plot- and catchment-scale simulations against field data (Cadini et al., 2013; Wang et al., 2014). Van Schaik et al. (2010) used data from plot-scale irrigation experiments to parameterize three soil profile models. They used these parameterized models to simulate plot-scale water balance and eventually compared this to the water balance observed at catchment scale. However, later work by van Schaik et al. (2014) relied on a different model requiring different parameters for 3D simulations of their catchment. For all these studies, it is difficult to fully assess the value of detailed simulations at plot scale for parameterizing catchment simulations. Moreover, the question of how spatial heterogeneity within

a catchment affects the simulation results at catchment scale in such an approach remains open: Does it matter how representative the used plot-scale observation of preferential flow is for the entire catchment? Or does the effect of locally different characteristics "smooth out" with scale, as observed, for example, for initial saturation (Zehe and Blöschl, 2004) and saturated hydraulic conductivities (Meyerhoff and Maxwell, 2011)?

We conducted a study on the transferability of plot-scale-derived preferential flow parameterization to catchment rainfall–runoff simulations for the Weierbach headwater (Luxembourg). We parameterized the preferential flow based on plot-scale observations during irrigation experiments and subsequently transferred the parameters to catchment-scale simulations. We used the integrated hydrological surface–subsurface model HydroGeoSphere (Therrien et al., 2010), which allowed us to use the same preferential flow representation (dual-permeability approach) at plot and catchment scales. By doing this, we hypothesized that model parameters and processes are scale invariant and that a direct extension of the model from plot to catchment scale is possible. We constrained the plot-scale parameters with observations from three irrigation experiments (dye tracer patterns, Br^- concentration profiles). We then tested the transfer of several preferential flow parameter sets from plot scale to the catchment-scale model and validated the catchment simulation results with discharge and soil moisture observations. The aim of this approach was to assess (i) the value of plot-scale irrigation experiments for identifying parameter sets for a realistic dual-permeability simulation at catchment scale, (ii) the effect of the spatial heterogeneity of the occurrence and prominence of vertical preferential flow (and thus the importance of the representativeness of the used plot-scale observation) on the parameter transfer, and (iii) the spatial (vertical and lateral) and conceptual representation of preferential flow with a dual-permeability approach for capturing the integrated signals of a humid-temperate catchment in long-term simulations.

Please note that, when referring to our simulations, we use the term *preferential flow* for describing the parameterization of nonuniform flow with a dual-permeability approach, focusing on the vertical preferential flow component that is introduced with this approach. In addition, the model setup consists of multiple soil layers with contrasting hydraulic conductivities, which enable a development of nonuniform lateral subsurface flow. This lateral flow can also be interpreted as preferential flow but is referred to here as fast or nonuniform lateral (subsurface) flow.

Study Site and Previous Work

The simulation of preferential flow is based on field investigations that were conducted in and near the Weierbach catchment, a forested 42-ha experimental catchment in the foothills of the Ardennes massif in the west of Luxembourg (Fig. 1). The area is characterized by shallow soils overlying periglacial deposit layers and Devonian slate bedrock (Juilleret et al., 2011; Moragues-Quiroga et al., 2017). Catchment runoff shows distinct differences between dry and wet catchment states, with single-peak hydrographs during dry and double-peak hydrographs (Martínez-Carreras et al., 2016) under wet conditions. The processes contributing to the distinct streamflow behavior have been under investigation for many years (Fenicia et al., 2014; Wrede et al., 2015; Klaus et al., 2015; Martínez-Carreras et al., 2016; Schwab et al., 2017). The common perception of these studies mainly relates the sharp, short-lasting (single-peak) hydrographs to flow paths on the surface and in the shallow (top)soil and the second, delayed peaks to the exceedance of storage thresholds, connecting deeper (ground)water.

Several studies around the Weierbach have investigated preferential flow. Irrigation experiments by Jackisch et al. (2017) on three 1-m^2 plots in the direct vicinity of the catchment (same vegetation and pedolithological structure, Fig. 1) showed fast vertical infiltration and preferential flow through a network of interaggregate pores. Scaini et al. (2017, 2018) observed that vertical subsurface flow and vertical preferential pathways dominated fluxes in the top 2 to 3 m during two irrigation experiments on a 64-m^2 hillslope section in the Weierbach catchment. In addition, Scaini et al. (2017, 2018) found indications of a fast connection between hillslope and stream, which they related to a fast lateral flow in the fractured bedrock 2 to 3 m below the surface. In a nearby catchment with the same pedolithological structure, Angermann et al. (2017) demonstrated for a hillslope that preferential flow paths developed in unsaturated soils shortly after the onset of intense irrigation or precipitation. Based on their investigations, they inferred fast lateral preferential flow through distinct paths at the interface of the periglacial deposit layer as one of the main processes in the hillslope, potentially contributing to the sharp, short-lasting (single) hydrograph peaks. In line with the field investigations, Glaser et al. (2016) suggested that incorporating preferential flow formulations could help to improve the performance of their physically based 3D single-domain HydroGeoSphere model of the 6-ha headwater of the Weierbach (Fig. 1). As highlighted in Fig. 1, their simulations notably missed some specific hydrograph responses of the broad, delayed peaks.

In this study, we relied on the 6-ha headwater HydroGeoSphere model of Glaser et al. (2016) and the information derived from the three 1-m^2 plot irrigation experiments of Jackisch et al. (2017) as the basis for the parameterization of preferential flow simulations at plot and catchment scale (see below). In addition, soil moisture was monitored from October 2012 to April 2014 on a hillslope in the catchment (Fig. 1) with time-domain reflectometers (Campbell CS650) installed horizontally at the 10-, 20-, 40-, and 60-cm depths. The stream level was measured at the outlet of the catchment (ISCO 4120 Flow Logger) and transformed into discharge via a rating curve. Additional discharge measurements (ISCO 4120 Flow Logger, transformation via a rating curve) were performed at the outlet of the upper 6-ha headwater region of the catchment (Fig. 1) starting in spring 2013.

The irrigation experiments were described in detail by Jackisch et al. (2017). Here, we briefly summarize the information relevant for
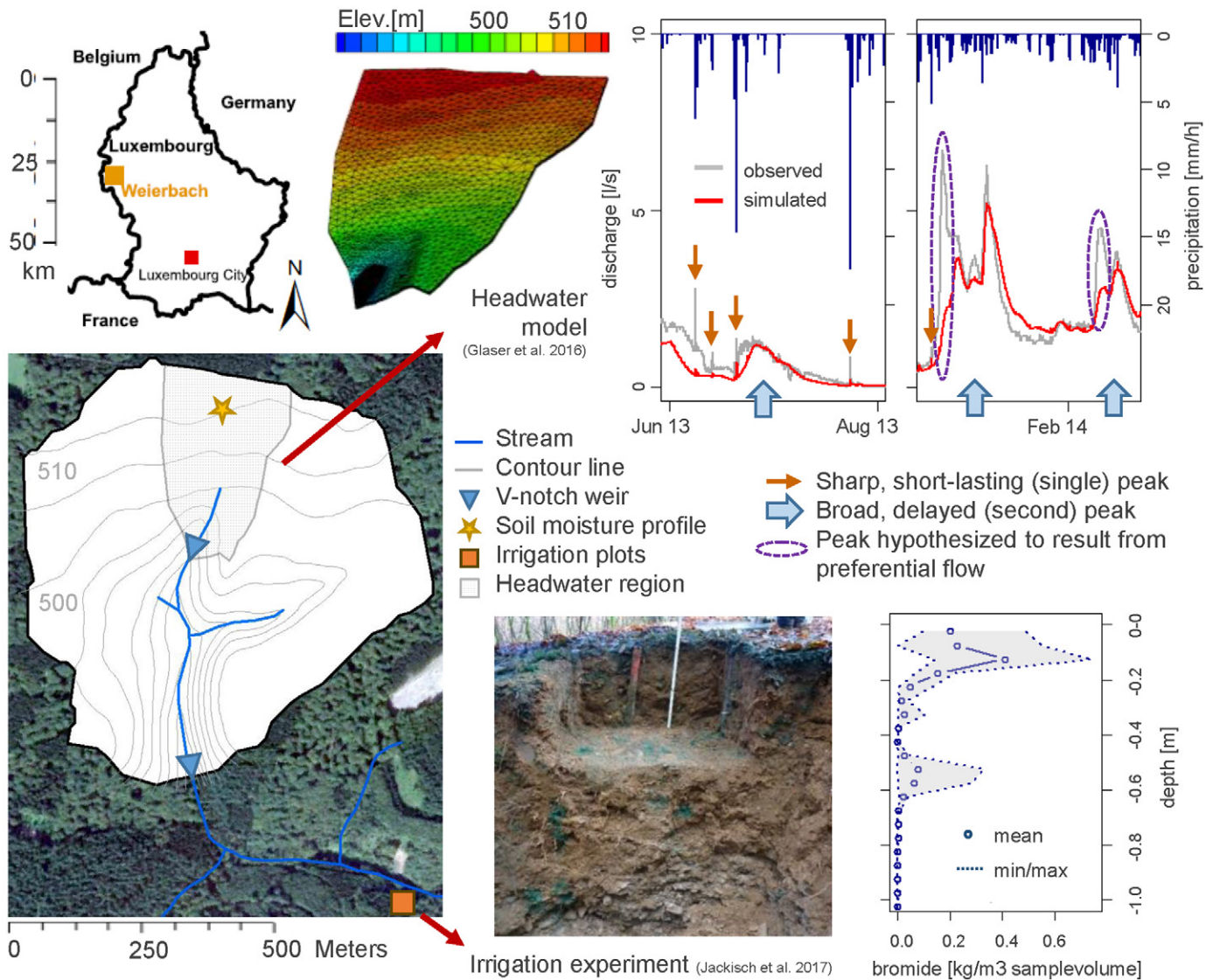
Fig. 1. Weierbach catchment and surroundings (left), model grid and hydrographs of the 6-ha headwater model from Glaser et al. (2016) (top right), and example excavation plot and Br⁻ depth profile of the irrigation experiments from Jackisch et al. (2017) (bottom right).

this study. Three 1-m² plots were irrigated for 1 h with 30 mm (Plot 2) or 50 mm (Plots 1 and 3) of water mixed with Br⁻ (5 g L⁻¹ KBr) and the dye tracer Brilliant Blue (4 g L⁻¹). At each plot, soil moisture was continuously measured with a time-domain reflectometry tube probe (IMKO IPH/T3) at 10-cm depth increments down to a depth of 1.2 m. Each plot was excavated 24 h after irrigation and analyzed for Brilliant Blue patterns (three vertical faces, five to seven horizontal faces) and vertical profiles of Br⁻ recovery (five vertical profiles with horizontal and vertical sample spacing of 5 cm down to a maximum depth of 1 m). The observed soil moisture responses, Brilliant Blue patterns, and Br⁻ concentrations consistently indicated a fast and pronounced nonuniform vertical transport down to the upper boundary of the periglacial deposit layer (starting at a depth of approximately 0.6 m, Fig. 1). Apart from that, the monitored soil moisture depth profiles and vertical patterns of dye and Br⁻ showed a high spatial heterogeneity within and between the different irrigated plots (Jackisch et al., 2017).

Modeling Approach
HydroGeoSphere model

HydroGeoSphere (Aquanty, 2015) is a 3D integrated hydrological surface—subsurface model code that can simultaneously solve a modified form of the Richards equation for transient flow in the subsurface domain and the diffusion wave approximation of the two-dimensional Saint-Venant equation for flow in the surface domain. Solute transport can be implemented with an advection–dispersion equation. Preferential flow can be considered via flow in discrete fractures or via a dual-permeability approach (Therrien et al., 2010; Aquanty, 2015).

In this study, we incorporated preferential flow with the dual-permeability approach. In this approach, two subsurface continua coexist. One continuum represents water flow and solute transport in the soil matrix (hereafter called the matrix domain); the other continuum represents flow and solute transport in the macropores (hereafter called the macropore domain). The two domains are

volumetrically partitioned on the total subsurface volume and parameterized independently with different soil hydraulic parameters (used here: saturated hydraulic conductivity K_s, porosity n, residual saturation θ_r, van Genuchten α, and van Genuchten β). Exchange between the matrix and macropore domains follows a dual-node approach, i.e., the interface between the two domains is represented as a very thin layer of porous material through which a Darcy flux is driven by respective hydraulic head differences between the two domains. Consequently, using the dual-permeability approach requires the definition of soil hydraulic parameters for the matrix and macropore domains as well as for the exchange interface. Additionally, fluid and mass exchange parameters for the exchange interface (fex, mex) and a parameter defining the macropore domain percentage on the total subsurface volume (pct, summing up to 100% with the matrix domain percentage) are needed.

The plot-scale and catchment-scale simulations of this study build on a modified HydroGeoSphere model of the 6-ha headwater region of the Weierbach as described by Glaser et al. (2016). They used the model to simulate coupled surface and subsurface flow from October 2010 to August 2014 with hourly precipitation and potential evapotranspiration forcing. A nested model grid (area of 6 ha, depth of 3 m) was composed of nine layers of three-sided prisms with vertical element heights ranging from 0.15 m (top layers) to 1 m (bottom layer) and horizontal element lengths ranging from 10 m (hillslope) to 0.25 m and less (riparian zone and stream bed) (Fig. 2, left). Eleven matrix domain zones were parameterized in the grid with differing hydraulic characteristics, representing a humic, dystric, skeletic, and siltic Cambisol at the hillslopes (Ah, B1, B2), a stagnic soil in the riparian zone (LP), and universally underlying layers of transition from subsoil to regolith (IIC), weathered bedrock (Cv), and solid slate (mC) (Fig. 2, middle). The matrix domain zones were implemented as laterally homogeneous layers all over the catchment with the exception of the outcropping of the soil layers and the overlying stagnic soil in the riparian zone.

Model parameterization relied on field observations, including electrical resistivity tomography and measurements of soil hydraulic parameters from soil samples, literature values, and trial and error calibration of porosities, hydraulic conductivities, and evapotranspiration parameters. The measurements used for parameterization did not explicitly exclude macroporous structures. The highly saturated hydraulic conductivities and the porosities of the soil and regolith layers (Table 1, Soil Zones 1–6) suggest that a macropore influence was already implicitly included in the matrix domain parameterization. This reflection was considered in the following dual-permeability parameterization, where we explicitly implemented vertical preferential flow by distinguishing between soil matrix and macropores. To incorporate the dual-permeability approach, we adapted the previous model as described below and simulated the plot-scale irrigation experiments and the hydrological catchment response for a period of 18 mo (October 2012–April 2014). For additional information on the basic model setup (e.g., evapotranspiration parameters, numerical controls), see Glaser et al. (2016).

Plot-Scale Model Setup

We simulated the three plot-scale irrigation experiments of Jackisch et al. (2017) in a horizontal 1-m^2 soil column of 6-m depth implemented in HydroGeoSphere. The grid was defined by 0.25-m^2 quadratic elements with element heights of 1 cm between the 0- and 4-m depths and element heights of 5 cm between the 4- and 6-m depths. Flow and transport were simulated in the subsurface only (no surface domain) because this can avoid numerical problems, and no surface runoff was observed during the experiments. We set up the matrix domain of the model column identically to the hillslope structure of Glaser et al. (2016), i.e., the soil type depth profile and parameterization of the hillslopes (Soil Zones 1–10; cf. Fig. 2, Table 1) was applied to the upper 4 m of the model column (Fig. 2). The lower 2 m of the model column (4–6 m) served as porous storage ($K_s = 1$ m d^{-1}, $n = 20\%$, $\theta_r = 0.02$,
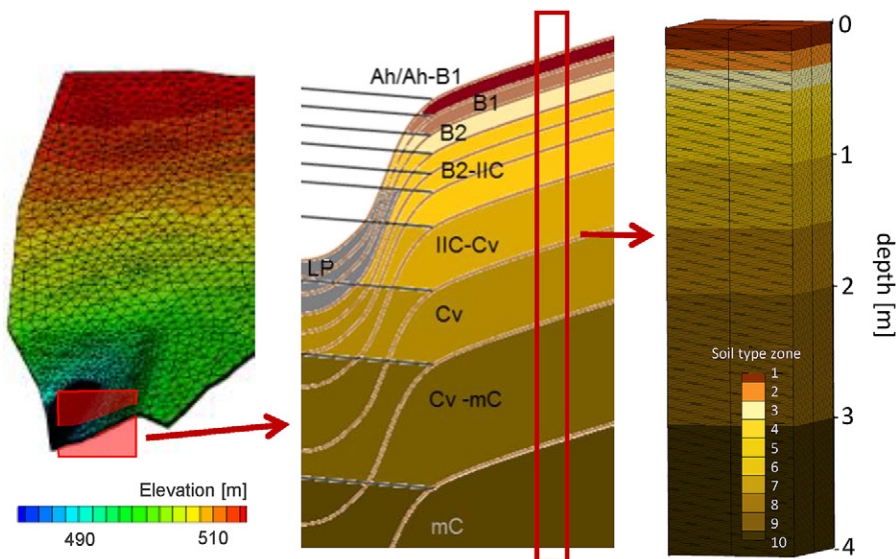

Fig. 2. Schematic cross-section through the subsurface setup showing the soil zones (middle) as defined in the headwater model grid of Glaser et al. (2016) (left) and in the plot-scale model grid (right) used for simulating the irrigation experiments. The cross-section has been modified from Glaser et al. (2016).

Table 1. Soil hydraulic parameters from the single-domain model of Glaser et al. (2016) including residual saturation (θ_r), van Genuchten parameters α and β, porosity (n), and saturated hydraulic conductivity (K_s). In this study, these values were used for the parameters of the matrix domain or as effective model parameters (for K_s and n only), respectively. (Table modified from Glaser et al., 2016).

Soil zone	θ_r	α	β	n	K_s
		m^{-1}			$m\,d^{-1}$
1 (Ah/Ah-B1)	0.12	6.6	1.46	0.74	1.71×10^1
2 (B1)	0.10	22.1	1.42	0.61	1.71×10^1
3 (B2)	0.10	22.1	1.42	0.45	4.59×10^1
4 (B2-IIC)	0.10	22.1	1.42	0.30	9.30×10^2
5 (B2-IIC)	0.10	22.1	1.42	0.15	2.04×10^3
6 (B2-IIC)	0.02	6.0	1.50	0.20	8.40×10^2
7 (IIC-Cv)	0.02	6.0	1.50	0.15	3.00×10^0
8 (Cv)	0.02	6.0	1.50	0.10	1.20×10^{-2}
9 (Cv-mC)	0.02	6.0	1.50	0.05	9.00×10^{-4}
10 (mC)	0.02	6.0	1.50	0.01	2.40×10^{-5}
11(LP)	0.10	22.1	1.42	0.61	7.80×10^0

$\alpha = 6\ m^{-1}$, $\beta = 1.5$) to prevent water from ponding at the bottom of the upper 4 m.

Preferential flow was incorporated in the upper 4 m by defining a macropore domain with the same soil zone layering as for the matrix domain. This required preferential flow parameters (K_s, n, θ_r, α, β, fex, mex, and pct) for 10 different soil type zones (cf. soil type zones of the matrix domain at the hillslopes, Fig. 2). These parameters were explored within a Monte Carlo approach (see below). Bromide transport was simulated with a tortuosity of 0.1, a diffusion coefficient of $1.6 \times 10^{-4}\ m^2\,d^{-1}$, and longitudinal and transverse dispersivities of $d_l = 0.05$ m and $d_t = 0.005$ m for the matrix and $d_l = 0.1$ m and $d_t = 0.01$ m for the macropore domain (cf. Gelhar et al., 1992; Rosenbom et al., 2009; Leistra and Boesten, 2010; Laine-Kaulio et al., 2014).

Following Laine-Kaulio et al. (2014), we partitioned the input fluxes (solute and water) at the upper boundary of the model between the macropore and matrix domain with a ratio of 90:10. We assigned no-flow boundaries to the sides and the bottom of the model column. Initial saturation was identical for the matrix and macropore domains (see Supplemental Material S1 for values); the initial Br^- concentration was set to zero ($10^{-15}\ kg\,m^{-3}$ to avoid numerical instabilities) in both domains.

Plot-Scale Simulation of Preferential Flow with a Monte Carlo Approach

We performed 20,000 brute-force Monte Carlo (MC) simulations for identifying the best-performing parameter sets for the three irrigation experiments. A total of 12,000 MC runs were simulated with an irrigation rate of 50 mm h^{-1} (representing Plots 1 and 3) and 8000 simulations were performed with an irrigation rate of 30 mm h^{-1} (representing Plot 2). The MC runs differed in the parameterization of preferential flow (parameters of the macropore domain and parameters for defining the partitioning and exchange between the matrix and macropore domain, cf. Table 2). Transport and matrix parameter values (Table 1) were kept constant with the exception of saturated hydraulic conductivity and porosity of the matrix domain. These two parameters were adapted in half of the MC simulations to account for the assumption that values used in the single-domain model implicitly included the effect of preferential flow (cf. high values in Table 1).

In total, 12 preferential flow parameters were needed for each of the 10 different soil type zones. Consequently, independent value variations for each parameter and soil layer would have resulted in 120 values to be modified per model run. To keep a reasonable number of parameter variations, we varied only 8 of the 12 preferential flow parameters. Precisely, the values of the hydraulic parameters θ_r, α, and β of the interface between the macropore and matrix domain and the residual saturation θ_r of the macropore domain were not varied in the MC runs (Table 2, no value variation). In addition, we reduced the number of necessary parameter variations by assigning a global value for all 10 soil layers for some parameters (fex, mex, and n) (Table 2, global values in depth profile).

The parameters α, β, K_s, and pct were subject to separate value assignment for different soil layers (Table 2, layer-specific values in depth profile). To avoid unrealistic hydraulic and capillary jumps and barriers, the value assignment was constrained to the form (value ratio) of several predefined nonuniform depth profiles. To define realistic depth profiles of parameters [hereafter labeled $dp_{xxx}(z)$], we applied different approaches (hereafter labeled DP_{xxx}) as multiple working hypotheses (Clark et al., 2011) that rely on field observations and their different interpretations (Table 2, Supplemental Table S1). Details on the different approaches DP_{xxx} and the pre-defined depth profiles $dp_{xxx}(z)$ obtained are described in Supplemental Material S1.

Briefly, different van Genuchten α and β values were assigned to the different soil layers based on two different macropore categories: biopores (b) and fractures (f). The macropore categories b and f were assigned to the different soil layers based on the characteristics observed in the excavated irrigation plots (DP_{cat}, dp_{cat}; Table 2, Supplemental Table S1). The depth profile dp_{pct} for the macropore percentage (pct) was parameterized with four different approaches DP_{pct} A to D (Table 2). The approaches DP_{pct} A and DP_{pct} B represented two different ways of interpreting the Brilliant Blue patterns observed at the irrigation plots, approach DP_{pct} C assigned a constant percentage with depth, and approach DP_{pct} D relied on results from preliminary test simulations (Supplemental Material S1, Supplemental Table S1). The saturated hydraulic conductivity of the macropores (K_s) was assigned separately to the different soil layers following two different approaches (DP_{Ks} A and B). The K_s value was calculated either based on macropore apertures (apert, which required the definition of macropore aperture depth profiles dp_{apert}, DP_{Ks} A, Table 2, Supplemental Table

Table 2. Definition and constraints of macropore and interface parameters in the MC simulations. Parameters were assigned globally or separately to different soil layers z. Variations of separately assigned values were dependent on several fixed depth profiles that were pre-defined with various approaches DP_{xxx}, A to D, partly requiring some additional adjunct parameters. The resulting predefined depth profiles dp_{xxx} are shown in Supplemental Table S1. Here, information is given on how the depth profiles and adjunct parameters were used for the definition of parameter values. Parameter values were modified either by randomly sampling them from a uniform distribution $U(a,b)$ or based on a randomly sampled modification factor F_{xxx}.

Parameter†	Value variation	Global or layer-specific values in soil layers z‡	Depth profile predefinition method§	Adjunct parameters	Parameter calculation¶	Value constraint¶	Rationale for constraint range
Macropore domain							
n	yes	g				$n \sim U(0.75,0.99)$	ensure $n > n_{\text{original}}$
θ_r	no	g				0.01	
$\alpha(z)$ (m⁻¹)	yes	l	DP_{cat}	$dp_{\text{cat}}(z) \rightarrow \{b,f\}$		$\alpha_b \sim U(2.5,30.0)$ $\alpha_f \sim U(1.0,10.0)$	literature (Köhne et al., 2002; Rosenbom et al., 2009; Kordilla et al., 2012; Laine-Kaulio et al.,2014)
$\beta(z)$	yes	l	DP_{cat}	$dp_{\text{cat}}(z) \rightarrow \{b,f\}$		$\beta_b \sim U(1.1,5.0)$ $\beta_f \sim U(1.1,5.0)$	
$pct(z)$	yes	l	DP_{pct} A–D		$F_{pct} \times dp_{pct}(z)$, $F_{pct} = 1/X$ or $F_{pct} = X$	$X \sim U(1.0,2.5)$	ensure $0 < pct < 0.95$
$K_s(z)$ (m d⁻¹)	yes	l	DP_{Ks} A–B / DP_{Ks} A	$apert(z)$ (m),DP_{apert} A–D	$apert(z)^2 \times 9.81/12 \times 86{,}400 \times 10^6$ / $apert(z) = 10^{F_{apert}} \times dp_{apert}(z)$	$F_{apert} \sim U(-2,1)$	arbitrary, ensure $10^{-7} < apert < 0.05$
			DP_{Ks} B	$K_{\text{s-matrix}}(z)$ (m d⁻¹)	$\{K_{\text{s-original}}(z) - [1 - pct(z)] \times K_{\text{s-matrix}}(z)\}/pct(z)$ $K_{\text{s-matrix}}(z) = 10^{F_{\text{matKs}}} \times K_{\text{s-original}}(z)$	$F_{\text{matKs}} \sim U(-4,0)$	$K_{\text{s-matrix}} < K_{\text{s-original}}$; lower boundary arbitrary
Interface							
fex (m⁻²)	yes	g			$10^{F_{fex}}$	$F_{fex} \sim U(-5,2)$	arbitrary
mex (d⁻¹)	yes	g			$10^{F_{mex}}$	$F_{mex} \sim U(-3,4)$	arbitrary
$K_s(z)$ (m d⁻¹)	yes	l			$10^{F_{\text{intKs}}} \times K_{\text{s-original}}(z)$	$F_{\text{intKs}} \sim U(-3,3)$	arbitrary
$\alpha(z)$ (m⁻¹)	no	l			$\alpha_{\text{original}}(z)$		
$\beta(z)$	no	l			$\beta_{\text{original}}(z)$		
$\theta_r(z)$	no	l			$\theta_{r\,\text{original}}(z)$		

† n, porosity; θ_r, residual saturation; α, β, van Genuchten parameters; K_s, saturated hydraulic conductivity; pct, percentage of total subsurface domain comprised of macropores; fex, flow exchange coefficient; mex, mass exchange coefficient

‡ g, global; l, layer specific.

§ DP_{cat}, method for defining a depth profile $dp_{\text{cat}}(z)$ of macropore types (biopores b or fractures f), which were subject to separate value assignments for α and β; DP_{pct}, four different methods A–D for predefining different depth profiles $dp_{pct}(z)$ for pct; DP_{Ks}, two methods A and B for defining $K_s(z)$: A relies on predefined depth profiles $dp_{apert}(z)$ of macropore apertures $apert(z)$ (following four predefinition methods DP_{apert} A–D), B relies on maintaining effective hydraulic conductivities as $K_{\text{s-original}}(z)$, thus requiring adapted matrix conductivities $K_{\text{s-matrix}}(z)$. (cf. Table 1).

¶ X_{original}, matrix parameter in the headwater model of Glaser et al. (2016) (cf. Table 1).

S1) or as a function of varied matrix conductivities $K_{s\text{-matrix}}$, maintaining the same effective hydraulic conductivities as originally assigned to the matrix domain (cf. Table 1), but via a different contribution of the matrix and macropores to the effective hydraulic conductivity. In the latter case (DP$_{K_s}$ B, Table 2, Supplemental Material S1), matrix porosities were also adapted in such a way that effective porosities equaled the porosity values as originally assigned to the matrix domain (Table 1).

Ultimately, we varied eight macropore parameters in the MC simulation (Table 2, value variation). In half of the MC runs, we additionally varied matrix conductivities and porosities (see above and Supplemental Material S1). Some of the value variations were conditioned by variations of adjunct parameters (macropore category b or f, macropore aperture apert, matrix hydraulic conductivity $K_{s\text{-matrix}}$) and different methods (DP$_{cat}$, DP$_{pct}$ A–D, DP$_{K_s}$ A–B, DP$_{apert}$ A–D) for defining parameter depth profiles dp$_{xxx}(z)$ (see Table 2, Supplemental Material S1). The values for the varied parameters n, α, and β were randomly altered based on a uniform distribution U(a,b) across a specific constraint range (a,b) as defined in Table 2. The remaining varied parameters K_s (of the macropore domain, matrix domain, and interface), pct, fex, and mex were calculated as functions of so-called parameter modification factors F_{xxx}. These modification factors F_{xxx} were introduced to allow random sampling for the parameter values across several orders of magnitude. The modification factors F_{xxx} were randomly chosen from a uniform distribution U(a,b) across a constraint range (a,b), which we individually defined for each parameter modification factor by following the rationale indicated in Table 2.

Furthermore, we used two different depth distributions of initial saturation in the MC simulations. Both depth distributions reflected the conditions at the beginning of the irrigation experiment. One profile reflected the soil moisture observed at several locations close to the irrigation plots (DP$_{sat}$ A, Supplemental Table S1). The second profile was derived from simulated soil moisture from Glaser et al. (2016) (DP$_{sat}$ B, Supplemental Table S1). The two different initial saturation depth profiles were divided evenly among the different MC runs (Supplemental Table S2).

Evaluation of Plot-Scale Simulations

The plot-scale simulations were evaluated based on the Br$^-$ concentrations. We evaluated the simulated depth profiles of Br$^-$ with the average observed Br$^-$ profiles (i.e., the average profiles of the five individual vertical profiles for each irrigation plot, corrected with the corresponding recovery rates, assuming a uniform error with depth) of the different irrigation plots (i.e., comparing the 8000 simulations with 30 mm h^{-1} irrigation intensity with the profile of Plot 2 and the 12,000 simulations with 50 mm h^{-1} irrigation intensity with the profiles of Plots 1 and 3). We used a combination of two Nash–Sutcliff efficiencies (NSEs) as the model quality criterion. We calculated one NSE for the concentration profile across the full extent of observed depths (NSE$_{total}$). We calculated the second NSE (NSE$_{Br\text{-peak}}$) for a specific depth section between

0.32 and 0.82 m where Br$^-$ showed increased concentration for all irrigation plots. This second NSE$_{Br\text{-peak}}$ was specifically used for assessing the model performance in terms of preferential transport down to the periglacial deposit layer (cf. Fig. 1) without biasing the assessment with the influence of high Br$^-$ concentrations originating from a uniform transport front in the soil matrix in the upper 0.3 m. The MC simulations were ranked according to each of the two NSEs, and the resulting two rank numbers for each model run were summed to a final performance rank number.

Transfer from Plot- to Catchment-Scale Simulations

We selected the 10 best performing parameter sets, the parameter set at the first quartile, the median, and the third quartile of performance for each of the three irrigation plots to be used for catchment-scale modeling. The resulting subset of 39 parameter sets was intended to reflect the diversity of plot-scale preferential flow parameter sets. Based on this, we tested the effect of variable preferential flow parameterizations on long-term catchment-scale simulations.

Each of the 39 selected parameter sets was used for a simulation of the hydrometric catchment response (i.e., soil moisture and discharge, no solute transport) for the 6-ha Weierbach headwater from October 2012 to April 2014. We set up a single-domain reference model based on the headwater model of Glaser et al. (2016). Compared with their model, we reduced the temporal resolution (daily instead of hourly meteorological input data, see below and Supplemental Material S2) and the spatial resolution (coarsened horizontal grid in the riparian zone and vicinity) to save computational costs once the dual-permeability approach was added to the reference model. We added the dual-permeability approach by defining a macropore domain for all soil type zones except the stagnic soil layer of the riparian zone (because its soil structure did not indicate preferential flow in the field).

To check whether a daily rather than an hourly resolution of meteorological input data would affect the study conclusions, we compared catchment simulations with hourly input and daily input data for six different parameter sets. To do this, we selected the parameter set for the single-domain reference model and five dual-permeability parameter sets that produced different discharge responses at catchment scale. Details on the comparison are given in Supplemental Material S2. In summary, visual comparison and model efficiency (NSE) showed that the reduced input time step had no relevant effect.

The coarsening of the spatial resolution affected only the horizontal grid spacing in the riparian zone and its vicinity and still ensured a nested grid, with finer grid cells in the riparian zone and stream bed compared with the hillslopes. A comparison between the original headwater model of Glaser et al. (2016) and the reference model showed that this grid coarsening did not visibly affect the discharge simulation (data not shown). However, the adaptation of the grid required a new spin-up for defining initial conditions, which we performed during the period from October 2010 to October 2012 (loop of three repetitions).

The performance of the catchment-scale simulations was evaluated with discharge and soil moisture measurements (Fig. 1) from October 2012 to April 2014. The soil moisture observed generally responded to incoming precipitation with fast and strong soil moisture increases in the topsoil and an increasingly damped response with depth. This behavior was consistent with other measurement profiles in the Weierbach catchment (data not shown), yet some differences exist between absolute moisture values. Hence, we based the catchment model evaluation for soil moisture on the temporal soil moisture dynamic at different depths by calculating the Spearman correlation between moisture observations and moisture simulations. Discharge performance was evaluated by calculating the overall NSE.

◆Results
Plot-Scale Simulations
Monte Carlo Simulation of Irrigation Experiments

Simulating the three plot-scale irrigation experiments without dual permeability reproduced the transport front down to the 0.3-m depth, but there was no Br^- transport into deeper soil layers (Fig. 3a). The 20,000 Monte Carlo simulations with varying preferential flow parameters resulted in diverse depth transport

of Br^-. Approximately 5% of the simulations (8.5% for Plot 1, 4.2% for Plot 2, 2.1% for Plot 3) modeled the Br^- depth profiles observed with $NSE_{total} > 0$ and $NSE_{depth} > 0$ (NSE for characteristic Br^- peaks between 0.32 and 0.82 m). Approximately 40% of the simulations (28% of Plot 1, 64% of Plot 2, 26% of Plot 3) did not reproduce any Br^- peaks in deeper soil layers (no local maxima with concentrations $\geq 0.05\ kg\ m^{-3}$ in the $0.32-0.82$-m depth) and in that regard did not perform better than a single-domain model.

The model performance of the 20,000 parameter sets was barely sensitive to the values of single parameters and the related modification factors F_{xxx} or depth profile predefinition methods DP_{xxx}, (cf. Table 2), respectively. Mass exchange coefficient mex (F_{mex}), matrix conductivity $K_{s-matrix}$ (F_{matKs}, DP_{Ks}), macropore percentage pct (DP_{pct}, F_{pct}), and initial saturation sat (DP_{sat}) showed some relation to model performance, but this did not allow the identification of unique, well-performing parameter values (Supplemental Fig. S2).

Characteristics of the Parameter Sets Transferred to Catchment Scale

The 10 best-performing preferential flow parameter sets of each irrigation plot (later used for the catchment-scale simulations) showed some variability within the simulation results and
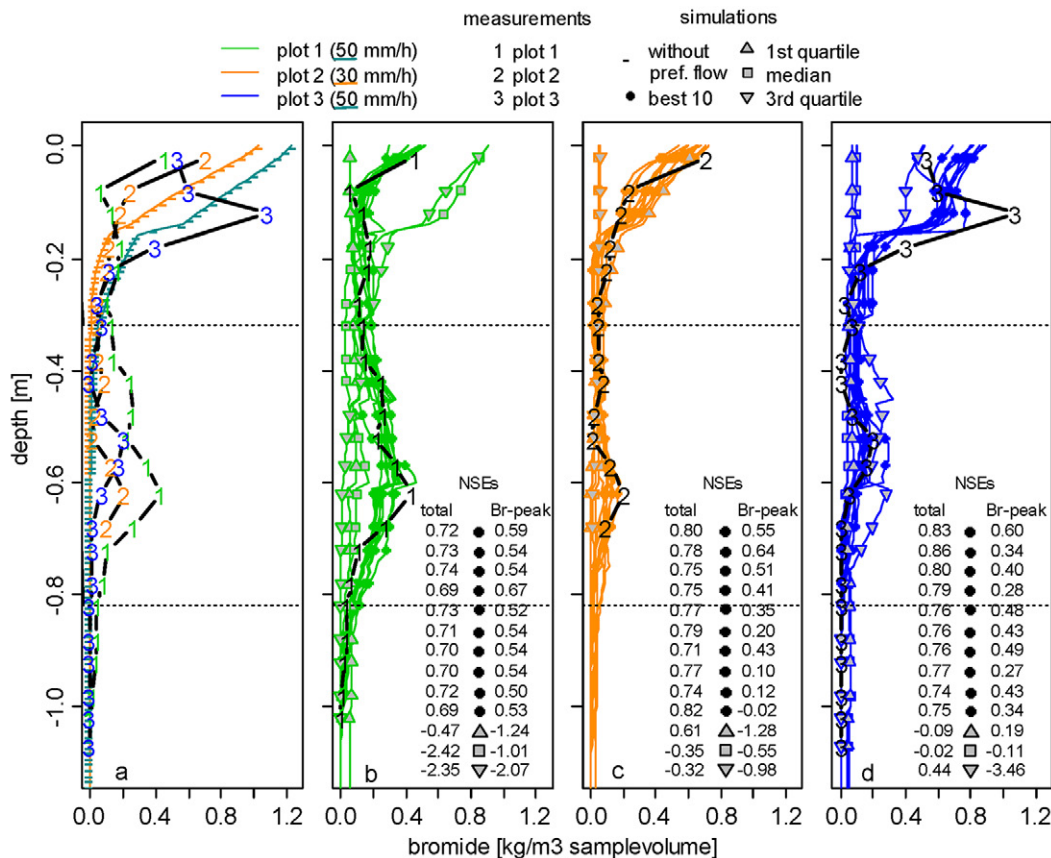

Fig. 3. Observed Br^- depth profiles of the three irrigation plots 1 to 3 (average profiles of five sampled vertical profiles, cf. Jackisch et al., 2017) in comparison to (a) simulations of the irrigation experiments without preferential flow and (b–d) simulations with a dual-permeability approach, showing the results of the 10 best, first quartile, median, and third quartile performing parameter sets of the Monte Carlo simulations for (b) Plot 1 (50 mm h^{-1} irrigation rate), (c) Plot 2 (30 mm h^{-1} irrigation rate) and (d) Plot 3 (50 mm h^{-1} irrigation rate).

the observations were not fully captured (Fig. 3b–3d). Nonetheless, the intraplot variability of the responses was low compared with the interplot variability, which was captured very well. The parameter sets with the first quartile, median, and third quartile of performance for each irrigation plot represented various nonfitting results, with simulations of more or less uniform Br⁻ depth profiles (e.g., Plot 2, third quartile, Fig. 3c), simulations with a transport front down to the 0.3-m depth (e.g., first quartile of Plot 2, Fig. 3c), or simulations with Br⁻ peaks in mismatching depths (e.g., Plot 3, third quartile, Fig. 3d).

The parameter values of the 39 parameter sets that were eventually transferred to catchment scale reflected the low parameter identifiability of the 20,000 parameter sets. The parameters that were not identifiable (n, α, β, apert, $K_{s\text{-int}}$, fex, cf. Supplemental Fig. S2) spread across most of the sampled parameter space for the 39 transferred parameter sets (Fig. 4). The resulting water retention curves also covered a large range of the tested shapes of retention curves (Supplemental Fig. S3). The parameter values and water

retention curves of the first, median, and third quartile model runs of each irrigation plot were not clearly separated from the values for the 10 best model runs (Fig. 4, Supplemental Fig. S3).

The values of the parameters that showed a relation to model performance (mex, $K_{s\text{-matrix}}$, pct, initial saturation sat; cf. Supplemental Fig. S2) extended only across a constrained part of the parameter space for the 10 best model runs of each irrigation plot, and the parameter values of the first, median, and third quartile model runs were more clearly separated from the best performing parameter sets. The modification factor for the mass exchange coefficient (F_{mex}) was spread across <50% of the sampled parameter space for the 10 best runs of all three irrigation plots (Fig. 4). Matrix conductivity was reduced for only two out of the 10 best runs of all three irrigation plots (F_{matKs}, Fig. 4, DP$_{Ks}$ A [no variation of $K_{s\text{-matrix}}$], Supplemental Table S3). The definition of initial saturation was based on soil moisture observations for the vast majority of the 10 best runs of all three irrigation plots (DP$_{sat}$ A, Supplemental Table S3). For pct, the restriction to a part of the parameter space was less distinctive. The depth profile predefinition method DP$_{pct}$ A (Brilliant Blue stains correspond to macropores) showed a tendency to be more common in the first quartile, median, and third quartile model runs than in the 10 best runs (Supplemental Table S3). In addition, the modification factor F_{pct} was limited to half of the sampled parameter space for the 10 best simulations of Plot 3 (Fig. 4).

Catchment-Scale Simulations
Discharge and Soil Moisture Responses

The reference catchment model adequately matched the observed discharge from October 2012 to April 2014 (NSE of 0.63). Nevertheless, the model showed clear limitations in reproducing some specific hydrograph responses (Fig. 5a, cf. also previous modeling by Glaser et al. [2016], Fig. 1). Several of the dual-permeability, catchment-scale simulations matched the observed hydrograph similarly to the reference simulation, with no improvement in the representation of the missing hydrograph features (Fig. 5b and 6, NSE > 0.5). All other dual-permeability simulations at catchment scale resulted in notably damped (Fig. 5c and 5d), flashy (Fig. 5c and 5f), or underestimated (Fig. 5e and 5f) discharge behavior and clearly could not reproduce the observed catchment discharge (Fig. 6, NSE < 0.5).

The differing performance of the simulated hydrographs was not related to the model performance of the parameter sets at plot scale. As an example, the top 10 performing parameter sets of Plot 1 showed a tendency to strongly underestimate catchment discharge (NSEs < −0.5, Fig.
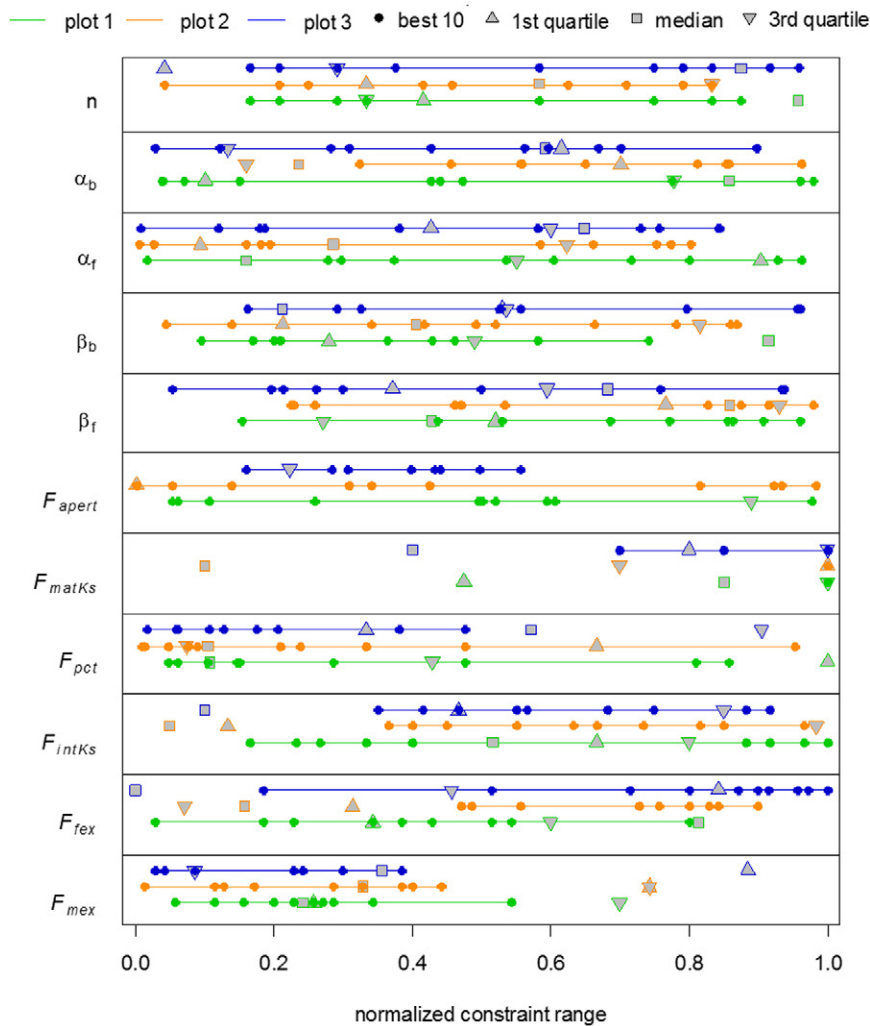

Fig. 4. Distribution of the parameter values and parameter modification factors of the 10 best, first quartile, median, and third quartile performing parameter sets of the MC simulations of the three irrigation plots. The values were normalized to the respective pre-constraint value ranges (Table 2), with 0 corresponding to the lowest and 1 to the highest constraint value.
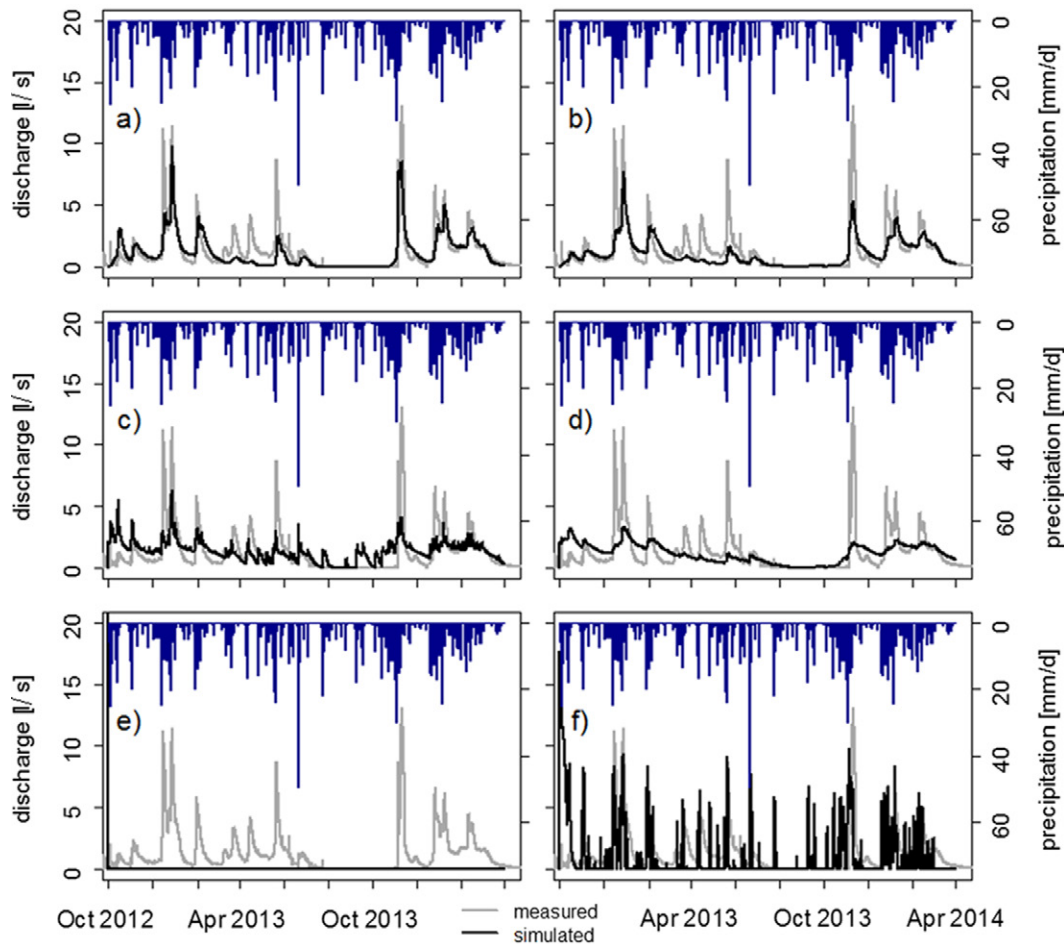
Fig. 5. Observed and simulated discharge for six simulations at catchment scale: (a) the reference simulation, (b–f) simulations with dual-permeability parameter sets from (b,d–f) the 10 best performing and (c) the first quartile performing parameter sets for Irrigation Plot 1.

6). However, the different hydrographs shown in Fig. 5b, 5d, 5e, and 5f all resulted from a parameter set belonging to the top 10 performing parameter sets of Plot 1. Also, the parameter set with the first quartile performance for Plot 1 resulted in a simulated catchment hydrograph with higher model efficiency than many simulations with parameter sets that belonged to the 10 best performing parameter sets at plot scale (Fig. 5c and 6). Thus, the performance of a distinct parameter set at plot scale was no predictor for its performance at catchment scale.

Soil moisture simulated with the reference model was similar to soil moisture observed in respect of the characteristic fast responses and a reduced responsiveness with increasing depth (Fig. 7a). The coefficients of correlation between simulated and observed soil moisture were >0.6 in all depths (Supplemental Fig. S4). Several of the dual-permeability simulations matched the soil moisture depth profiles observed in a similar way to the reference simulation with correlation coefficients > 0.6 for most depths (Fig. 7b and 7d, Supplemental Fig. S4). The parameter sets that resulted in such a similar soil moisture behavior were—for the most part—the same parameter sets that showed well-simulated hydrographs (NSE > 0.5, cf. Fig. 6, Supplemental Fig. S4). The remaining parameter sets resulted in soil moisture dynamics with

a poorer match of observed soil moisture (Fig. 7c, 7e and 7f, correlation coefficients <0.6 in most depths, Supplemental Fig. S4).

Parameter Sensitivity

The analysis of the parameter variations revealed a clear relation between model performance (hydrograph NSE) and the modification factor of the macropore aperture depth profiles F_{apert}. This factor modified the predefined macropore apertures that were used for the conductivity determination method DP_{Ks} A (cf. Table 2). The positive correlation identified between F_{apert} and hydrograph NSE (Fig. 8a) indicates that the model performed better with smaller macropore apertures and thus lower macropore conductivities at catchment scale, while such an effect was not observed at plot scale (cf. Fig. 4, Supplemental Fig. S2). The macropore conductivities that were determined based on method DP_{Ks} B, and thus relied on reduced matrix conductivities ($F_{matKs} < 0$), yielded mid-level performance for the catchment simulations (Fig. 8b). This was consistent with plot-scale behavior (cf. Supplemental Fig. S2). The effective hydraulic conductivities were very similar to the hydraulic conductivities of the reference model in the upper seven soil zones for all model runs resulting in hydrograph NSEs > 0 (Fig. 8c). In the lowest three soil zones, the effective conductivities were more variable (Fig.
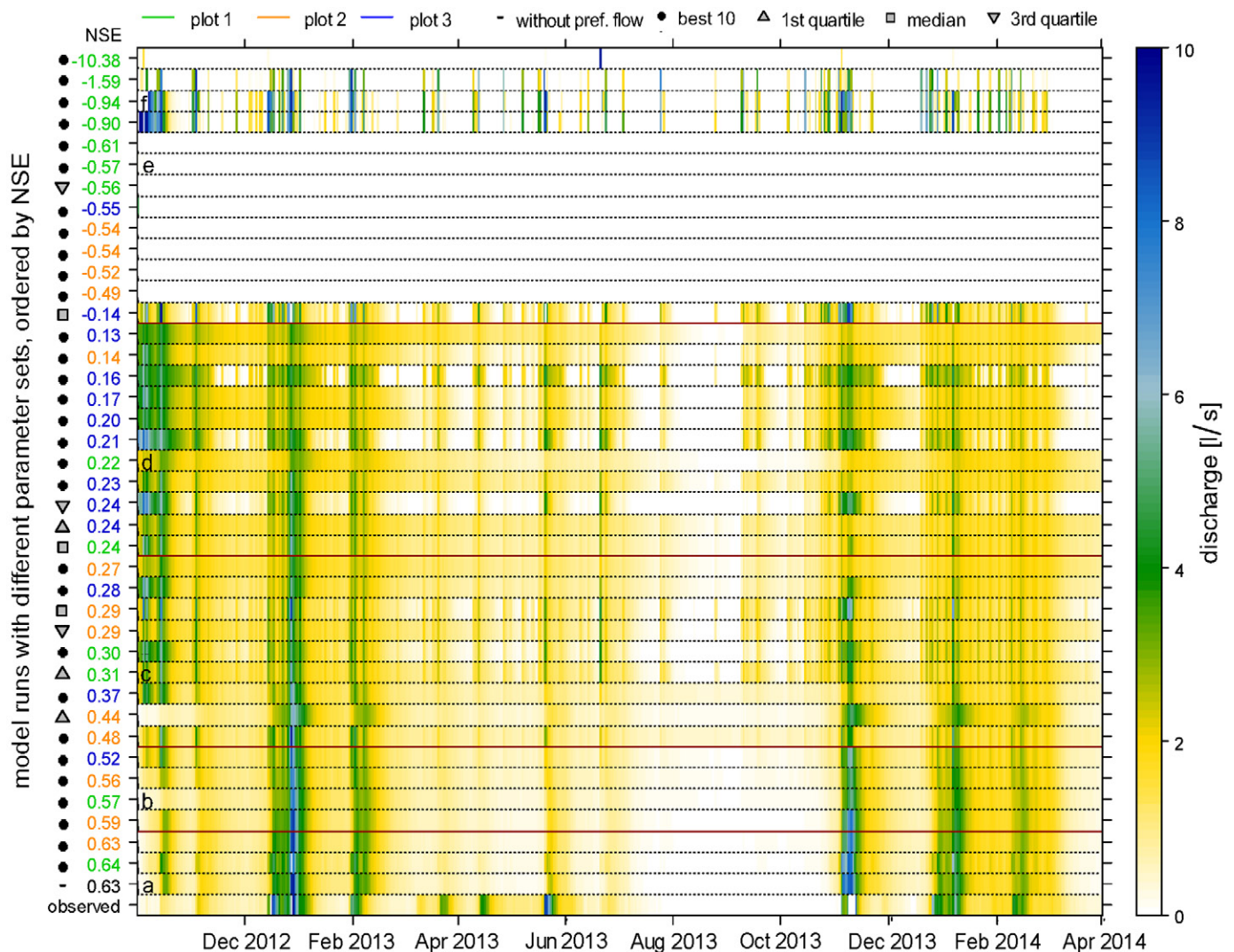
Fig. 6. Heat map showing observed and simulated discharge at catchment scale. Each row corresponds to one hydrograph; the magnitude of discharge is indicated with a color scale. The bottom row is the observed discharge, rows a through f represent the hydrographs of Fig. 5. The hydrographs are sorted according to their Nash–Sutcliffe efficiency (NSE). The colors of the NSE values indicate which irrigation plot was simulated with the parameter set at plot scale. The symbols correspond to the performance of the parameter sets at plot scale.

8d), but in all soil zones (1–10) the effective conductivities were distinctly higher when the model run resulted in a hydrograph NSE < 0. None of the other varied parameters showed any relation between their value and the model performance at catchment scale (Supplemental Fig. S5). This includes the parameters that showed some effect on plot-scale performance (i.e., macropore percentage and initial saturation, cf. Supplemental Fig. S2; note that the mass exchange coefficient was irrelevant for the catchment-scale model because only hydrometric responses were simulated).

⬥ Discussion and Conclusions
Value of Plot-Scale Observations for Parameterizing Dual-Permeability Catchment Simulations
Non-uniqueness of Plot-Scale Parameter Values

One aim of this study was to test whether the plot-scale irrigation experiments contained valuable information for parameterizing a dual-permeability catchment model. The MC simulation allowed us to find various preferential flow parameterizations that matched the plot-scale observations well. However, different preferential flow parameter sets resulted in equally good simulations, and we could not identify unique well-performing parameter values. Moreover, none of the different, partly contrasting approaches for predefining parameter depth profiles (DP_{pct}, DP_{Ks}, DP_{apert}) resulted in better simulation results than other approaches. This shows that it was not meaningful to identify the shape of the parameter depth profiles from our field observations.

The pronounced parameter non-uniqueness is consistent with other studies modeling preferential flow (e.g., Klaus and Zehe, 2010; Arora et al., 2012). Search algorithms for inverse parameter estimation that are more sophisticated than the applied brute-force Monte Carlo could allow a more efficient identification of optimal plot-scale parameterizations. However, this cannot solve the problem of parameter non-uniqueness and insensitivity (cf.
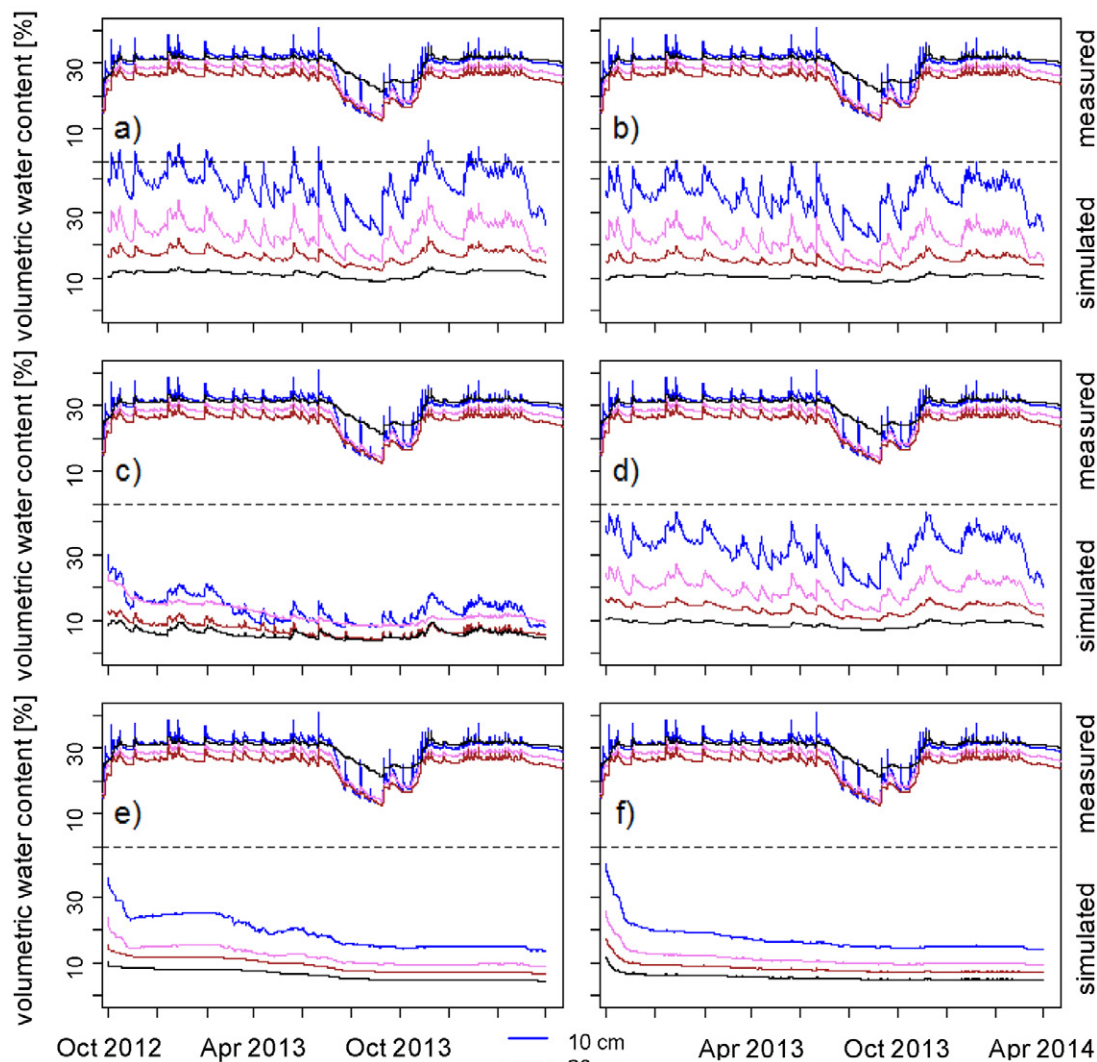
Fig. 7. Observed (top) and simulated (bottom) soil moisture at different depths for six simulations at catchment scale: (a) the reference simulation, (b–f) simulations with dual-permeability parameter sets from (b,d–f) the 10 best performing and (c) the first quartile performing parameter sets for Irrigation Plot 1 (cf. Fig. 5, Supplemental Fig. S4).

Jarvis et al., 2007; Arora et al., 2011, 2012). Additional observation data could help to better constrain the parameter values. For example, Larsbo and Jarvis (2005, 2006) analyzed the information content of solute concentrations in effluent fluxes, resident solute concentrations in the soil, drain flow, and soil water content to identify several parameters of a dual-permeability model. Their results showed that a combination of multiple observation data and measurements with high frequencies at the beginning of irrigation experiments were best for conditioning the parameterization. Furthermore, applying not only conservative tracers (as, e.g., Br^-) but also several reactive solutes with differing transport characteristics, such as weak or strong vs. intermediate sorptivity, could give information about the partitioning of fluxes between matrix and macropore flow (McGrath et al., 2009, 2010) and thus could help to better constrain the model parameters.

Nevertheless, the aim of this study was not to perform a detailed parameter identification and sensitivity analysis for dual-permeability simulations of the plot-scale irrigation experiments but rather to explore model performance at catchment scale for several parameter sets that were performing well at plot scale. In this context, we observed that different parameter sets with very similar, good fits at plot scale (i.e., the 10 best parameter sets) resulted in clearly different simulations of catchment discharge and soil moisture (cf. Fig. 6, Supplemental Fig. S4). This shows that a parameter set identified as optimal at plot scale does not necessarily perform well at catchment scale and that transferring one optimal parameter set from plot to catchment scale is problematic. Consequently, the robustness of the transferred parameter set needs to be validated against catchment-scale data or a direct parameter calibration at catchment scale is needed.

Effect of Spatial Heterogeneity of Vertical Preferential Flow on Catchment-Scale Simulations

Simulated catchment discharge and soil moisture showed similar variability among simulations independently of the irrigation experiment that was used for identifying dual-permeability
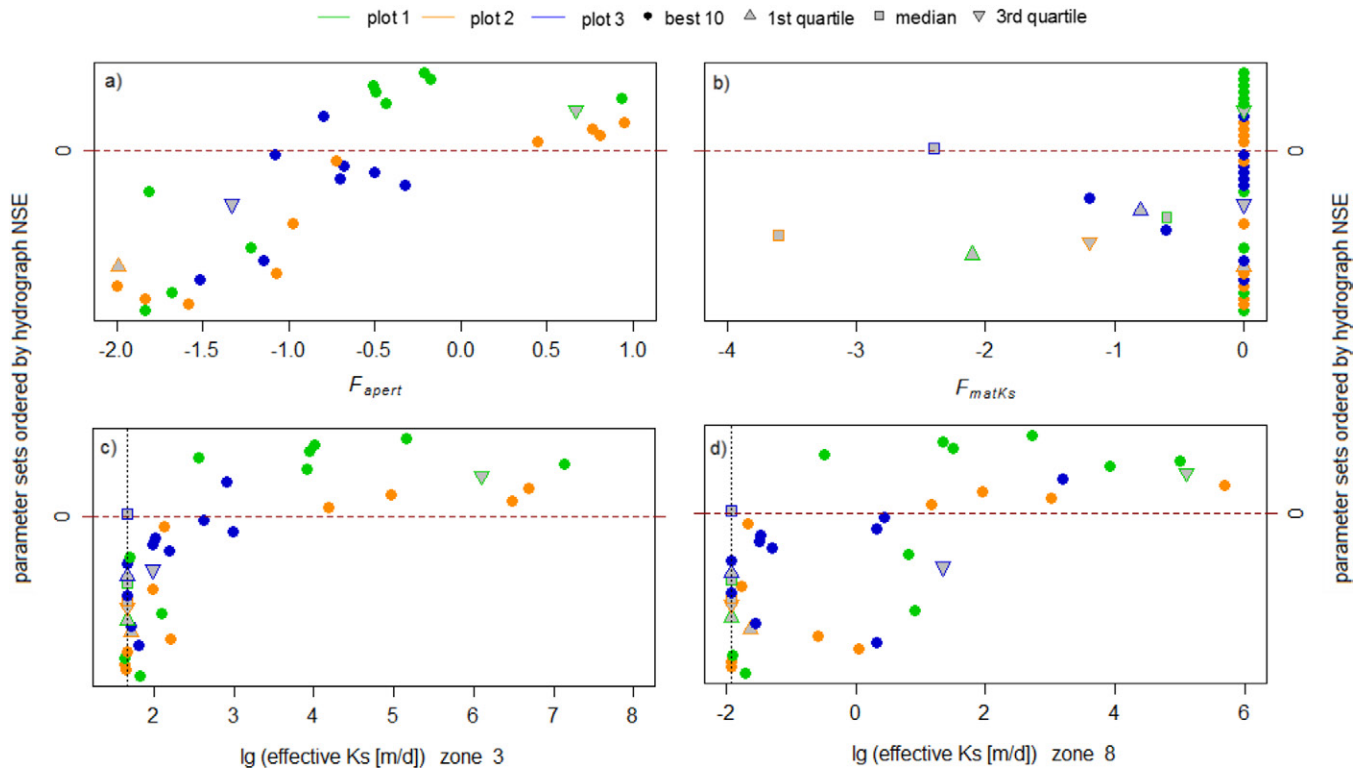
Fig. 8. Distribution of the parameter modification factors for (a) macropore aperture (F_{apert}) and (b) matrix hydraulic conductivity ($F_{\mathrm{mat}Ks}$) as well as of the effective hydraulic conductivity in (c) soil type Zone 3 and (d) soil type Zone 8 (cf. Fig. 1) within the catchment-scale simulations. Data points are sorted along the y axis according to the hydrograph Nash–Sutcliffe efficiency (NSE) of the parameter set (cf. Fig. 6). Data points above the red line correspond to parameter sets that resulted in a hydrograph NSE < 0, data points below the red line correspond to parameter sets that resulted in a hydrograph NSE > 0. The colors of the data points indicate which irrigation plot was simulated with the parameter set at plot scale. The symbols correspond to the performance of the parameter sets at plot scale.

parameter sets (cf. Fig. 6, Supplemental Fig. S4). Because the inter-plot variability among the three irrigation plots originated from a different degree of vertical preferential flow, it seems that the effect of spatial heterogeneity of vertical preferential flow between the plot-scale experiments averaged out at catchment scale. Thus, it was possible to condense spatial heterogeneity into average, effective values for the catchment scale. On the one hand, this is consistent with earlier studies that concluded that the effect of the spatial heterogeneity of initial soil moisture (Zehe and Blöschl, 2004), of hydraulic conductivity fields (Meyerhoff and Maxwell, 2011), or of pipe flow networks (Weiler and McDonnell, 2007) averaged out for the integrated hydrological catchment response. On the other hand, this is different from what was expected in studies discussing the role of the small-scale heterogeneity of preferential flow within a catchment (e.g., Christiansen et al., 2004; Graham and Lin, 2011; Liu and Lin, 2015; Wiekenkamp et al., 2016).

One might argue that a spatially homogeneous model setup works well only for simulating discharge. Certainly, it is not possible to capture the observed interplot variability among the three irrigation plots with average, effective values that are assigned homogeneously for all the catchment. However, the quality of the soil moisture evaluated as an internal response of the catchment model was also independent of the irrigation plot that was used to determine the model parameters. Potentially, the soil moisture simulation

may behave differently at various locations, which could lead to an improved realism at locations other than the soil moisture locations evaluated. Yu et al. (2014) demonstrated that simulated groundwater tables matched field observations well only when preferential flow and spatial subsurface heterogeneity were considered. Accordingly, it could be evaluated if and how the simulation of soil moisture would improve if a spatially more heterogeneous distribution of soil types in the model would be accounted for. Such a setup could potentially also result in a better prediction of the hydrograph response. However, including more spatial heterogeneity also increases the number of parameters and thus the degrees of freedom, which in turn increases the risk of overfitting the model. This is especially a problem if spatially heterogeneous parameters cannot be related to obvious differences observed in the landscape, such as different soil types. In the Weierbach catchment, such spatial differences in soil types are, with the exception of the riparian zone, not observable.

Representation of Preferential Flow at Plot and Catchment Scales
Adequacy of the Dual-Permeability Approach

Our study is one among several that has successfully applied the dual-permeability approach for simulating plot-scale observations of solute transport (e.g., Roulier et al., 2006; Arora et al., 2011; Cadini et al., 2013; Wang et al., 2014). The dual-permeability

approach allowed us to simulate the Br⁻ depth profiles for the three different irrigation experiments, whereas a single-domain approach did not reproduce the Br⁻ peak observed in deeper soil layers. In contrast to the plot scale, the best performing simulations with a dual-permeability approach at catchment scale, when transferring plot-scale parameters to the catchment-scale model, were very similar to the results of the reference simulation with a single permeability domain. This suggests that the incorporation of the dual-permeability approach did not improve the representation of the processes that are relevant for simulating the observed soil moisture and discharge response of the Weierbach catchment. Even more, the model performance for soil moisture and discharge decreased for many of our tested dual-permeability parameter sets.

Such a performance decrease when applying a dual-permeability model has not to our knowledge been reported in the literature so far, as it does not appear in cases where the parameters are calibrated at catchment scale. In line with our findings, Christiansen et al. (2004) and De Schepper et al. (2015) showed that the performance of their discharge and groundwater head simulations did not notably improve when including preferential flow in their models. Other studies could—at least partly—improve the simulation of internal, distributed (water tables and soil moisture) and integrated (runoff) responses when preferential flow was incorporated (dual permeability and other approaches) in their catchment models (Beckers and Alila, 2004; Zhang et al., 2006; van Schaik et al., 2014; Yu et al., 2014).

Obviously, the choice of a modeling approach for simulating preferential flow processes depends on the underlying question. If one is interested in the spatial patterns of preferential flow or in detailed analyses of exchange processes between macropores and soil matrix, an explicit implementation of macropore or fracture geometries and distributions (e.g., Vogel et al., 2006; Rosenbom et al., 2009; Klaus and Zehe, 2011; Jackisch and Zehe, 2018) and a conceptually different description of the pore-scale processes (e.g., Beven and Germann, 2013; Scheibe et al., 2015; Jackisch and Zehe, 2018) is necessary. In our case, we aimed to test a direct parameter transfer from plot to catchment scale. This requires a model approach that treats the processes at plot and catchment scales in the same way. The dual-permeability approach as implemented in HydroGeoSphere allows this. Because the dual-permeability approach was adequate for reproducing the three plot-scale irrigation experiments, we assume that it was also an adequate approach for the catchment scale. However, we did not test whether a different approach for simulating vertical preferential flow processes would have improved our simulation results at catchment scale.

Vertical vs. Lateral Flow in the Weierbach and Beyond

The lack of improved model efficiency in this study when incorporating preferential flow with a dual-permeability approach may be explained with a different relative importance of vertical and lateral flow at the different scales. At plot scale, vertical preferential flow (incorporated with dual permeability) was necessary to simulate the Br⁻ depth profiles observed. At catchment scale, model performance was highest for parameter sets where

the influence of vertical preferential flow (i.e., macropore conductivities) was low and homogeneous fast vertical infiltration was ensured with effective hydraulic conductivities, with values being similar to the conductivities of the single-domain reference model (cf. Fig. 8). Moreover, the model performed better when the matrix conductivity was not too low. This is manifested by the fact that the parameter sets with retained effective hydraulic conductivities but reduced matrix conductivities (cf. DP$_{Ks}$ B) resulted in catchment simulations with mid-level performance. This relation between model performance and parameter values indicates that the conceptual setup of the reference model was not improved by the incorporation of the dual-permeability approach. The reference model was composed of multiple soil layers with contrasting hydraulic conductivities (highest conductivities in Soil Zones 4–6, the depth where Br⁻ peaks were observed), allowing fast lateral subsurface flow along the interfaces between specific soil horizons. Thus, the modeling results indicate that uniform fast vertical flow in the unsaturated zone combined with connected fast lateral subsurface flow are the flow processes that mainly control the hydrometric response in the Weierbach catchment.

The role of fast lateral (preferential) flow on runoff generation has been widely observed (e.g., Weiler and McDonnell, 2007; Anderson et al., 2009; Yu et al., 2014; Laine-Kaulio et al., 2014; Wilson et al., 2016). Our results suggest that the relative importance of fast lateral flow on runoff generation largely outweighs the relative importance of vertical preferential flow. The likely reason for this not having been previously reported is that the few studies that explicitly compared catchment runoff simulations with and without preferential flow did not introduce vertical preferential flow and fast lateral flow through certain soil structures separately (i.e., layers, fractures, and macropores) (Beckers and Alila, 2004; Zhang et al., 2006; Yu et al., 2014) or were performed in a different climate (van Schaik et al., 2014). Only Christiansen et al. (2004) and De Schepper et al. (2015) compared a single-permeability domain model that included multiple soil layers with differing hydraulic conductivities (allowing for nonuniform lateral subsurface flow) with an equivalent dual-permeability model (maintaining similar effective hydraulic conductivities but allowing additional vertical preferential flow) for a climate similar to our study site. Consistent with our results, they also could not show a clear improvement of the overall runoff simulation.

The approach to derive catchment model parameters from detailed plot-scale simulations implies that the properties and processes that are relevant at small (plot) scale are also critical at catchment scale. According to our interpretation of our results, this seems not to be the case, since the results suggest that vertical and lateral flow play a different role at plot and catchment scales. Thus, a transfer of parameters for vertical preferential flow is not only problematic due to parameter non-uniqueness (cf. above) but also due to the fact that catchment response may be controlled by different process combinations than the plot-scale response. Certainly, our interpretation relies only on results derived with one specific modeling approach for one specific catchment. Yet, the

interpretation is consistent with the conceptual idea that processes and structures can have a different role at different scales (cf. Vogel and Roth, 2003), which is also supported by direct process observations (e.g., Jackisch et al., 2017). This concept suggests that details of structures that are important for processes at small scales can be integrated as averaged, effective descriptions in the representation of a structure that is relevant at larger scale. With respect to our results, this would mean that small-scale vertical preferential flow features can be integrated as averaged, effective descriptions for the modeling of the hydrometric response at larger scales. In other words, it would mean that the often discussed integrated effect of preferential flow on runoff and soil moisture at catchment scale (Beven and Germann, 2013; Weiler, 2017) could, in our case, be reflected in a combination of fast vertical infiltration and fast lateral subsurface flow in certain soil layers under certain conditions.

Limitations and Needs of Further Research

Limitations of the Modeling Approach

Our findings and their interpretation result from one specific modeling approach, i.e., a dual-permeability approach that was applied to a spatially homogeneous model setup. This means that a generalization of the results is limited. We especially do not intend to state that vertical preferential flow does not play any role in the distribution of soil moisture and on runoff generation. It is possible that a different model setup or conceptualization (e.g., governing equations of preferential flow, spatial variability) could have improved the hydrometric catchment response. Moreover, the dual-permeability approach improved the internal realism of the catchment simulations because it was able to reproduce the plot-scale observations. Yet, there are indications that the relative importance of vertical preferential flow for simulating hydrometric responses at catchment scale was less pronounced than suggested by the plot-scale observations. Instead, it was more important to properly account for a general fast infiltration in combination with nonuniform lateral flow. Therefore, depending on the model application, it is important to decide whether it is necessary to incorporate vertical preferential flow, as it comes with an additional parameterization effort and additional computational costs.

One limitation of our approach is the number of tested parameter sets at catchment scale. The total number of 39 simulations with different parameter sets for preferential flow is high compared with other modeling studies (e.g., Beckers and Alila, 2004; Weiler and McDonnell, 2007; van Schaik et al., 2014; Yu et al., 2014) and allowed us to analyze the effect of the parameter values spreading across the whole parameter space on catchment response. However, the applied approach, where several plot-scale parameter sets were transferred directly to catchment scale, does not fully analyze the parameter space at catchment scale. One may argue that other parameter sets may improve the integrated hydrometric response at catchment scale while also performing well at plot scale. Thus, further research on an inverse calibration of a physically based 3D dual-permeability catchment model with a subsequent validation of the identified parameters at plot scale is needed.

Another limitation is that we simulated solute transport only at plot scale, although solute transport is often one of the main reasons for incorporating preferential flow. However, we think that Br^- transport and water flow are similar enough (cf. Zehe and Blöschl, 2004) to investigate the transferability of parameter sets from plot scale to catchment models. Certainly, the impact of the dual-permeability approach on solute transport toward the catchment outlet and on catchment travel times remains unclear. Using a numerical experiment, Christiansen et al. (2004) found that the incorporation of preferential flow paths had a significant effect on the transport of reactive solutes, while the effect on the transport of conservative solutes (such as Br^-) was small. Relating this to the present study, it might be that the simulation of solute concentrations at the catchment outlet is impacted by a dual-permeability approach (positively or negatively). An analysis of this requires appropriate field data to validate the correctness of simulated solute transport at catchment scale, which was available neither in this study nor in the study of Christiansen et al. (2004). Hence, future work should evaluate the effect of the proposed approach on solute transport at catchment scale, as our results are restricted to the hydrometric response.

Generalizing our Results to Other Landscapes

We performed our study for one particular catchment. The subsurface structure of this catchment is characterized by shallow soils, highly permeable periglacial layers, and fractured slate. Preferential flow probably occurs in a particular network of interaggregate pores (Jackisch et al., 2017) and along imbricated clasts and fractures (Scaini et al., 2017). Plot and hillslope field studies further suggested that there is a substantial vertical preferential flow component (Jackisch et al., 2017; Scaini et al., 2017). Nonetheless, for the particular pedolithological structure of the Weierbach catchment, the performance of the simulations of catchment discharge and soil moisture did not improve when we explicitly accounted for vertical preferential flow. In line with this, for a catchment with a similar pedolithological structure, Loritz et al. (2017) showed that it was sufficient to include fast infiltration and connected lateral subsurface flow paths in a representative hillslope model for simulating the rainfall–runoff behavior.

In catchments with different physiographic settings, a more explicit representation of vertical preferential flow may have a stronger influence on hydrometric catchment responses. In agricultural soils with fine matrix textures and high amounts of biopores, such as earthworm burrows (e.g., Klaus et al., 2013), the influence of vertical preferential flow, as opposed to nonuniform lateral flow, on runoff generation may be much higher. Glacial till soils may be more similar to the structure of the Weierbach catchment, and Jansson et al. (2005) made conclusions in line with our study when comparing simulations of soil moisture in a glacial till soil with a one-dimensional single-domain and a two-domain model. Catchments with a climate different to Luxembourg can be more prone to a high importance of vertical preferential flow on runoff generation. This was shown by van Schaik et al. (2014), who improved hydrometric responses for simulations with preferential flow under semiarid conditions. Runoff

generation in catchments with slow velocities and short travel distances of lateral subsurface flow (cf. Klaus and Jackson, 2018) may also be less dominated by lateral subsurface flow, and the role of vertical preferential flow may become more important. Nonetheless, our findings highlight that the observation of vertical preferential flow in plot or hillslope experiments is not necessarily critical for improving catchment simulations of the hydrological response. Instead, some features that are easier to determine (e.g., multiple soil layers with contrasting hydraulic properties and effective conductivities) may be more important for understanding the structures and processes that are critical for water flow at catchment scale.

Supplemental Material

The supplemental material comprises a detailed description of the parameter depth profiles used in the MC simulations (Supplemental Material S1), the comparison of discharge simulations with hourly and daily meteorological input data (Supplemental Material S2) and supplemental result data (Supplemental Material S3) showing the distribution of all parameters compared to the performance of all plot-scale and catchment-scale simulations, the used water retention curves, and the correlations between simulated and observed soil moisture.

Acknowledgments

References

Angermann, L., C. Jackisch, N. Allroggen, M. Sprenger, E. Zehe, J. Tronicke, et al. 2017. Form and function in hillslope hydrology: Characterization of subsurface flow based on response observations. Hydrol. Earth Syst. Sci. 21:3727–3748. doi:10.5194/hess-21-3727-2017

Anderson, A.E., M. Weiler, Y. Alila, and R.O. Hudson. 2009. Dye staining and excavation of a lateral preferential flow network. Hydrol. Earth Syst. Sci. 13:935–944. doi:10.5194/hess-13-935-2009

Aquanty. 2015. HydroGeoSphere: A three-dimensional numerical model describing fully-integrated subsurface and surface flow and solute transport. User guide. Aquanty Inc., Waterloo, ON, Canada.

Arora, B., B.P. Mohanty, and J.T. McGuire. 2011. Inverse estimation of parameters for multidomain flow models in soil columns with different macropore densities. Water Resour. Res. 47:W04512. doi:10.1029/2010WR009451

Arora, B., B.P. Mohanty, and J.T. McGuire. 2012. Uncertainty in dual permeability model parameters for structured soils. Water Resour. Res. 48:W01524. doi:10.1029/2011WR010500

Beckers, J., and Y. Alila. 2004. A model of rapid preferential hillslope runoff contributions to peak flow generation in a temperate rain forest watershed. Water Resour. Res. 40:W03501. doi:10.1029/2003WR002582

Beven, K., and P. Germann. 2013. Macropores and water flow in soils revisited. Water Resour. Res. 49:3071–3092. doi:10.1002/wrcr.20156

Cadini, F., J. De Sanctis, I. Bertoli, and E. Zio. 2013. Upscaling of a dual-permeability Monte Carlo simulation model for contaminant transport in fractured networks by genetic algorithm parameter identification. Stochastic Environ. Res. Risk Assess. 27:505–516. doi:10.1007/s00477-012-0595-8

Christiansen, J.S., M. Thorsen, T. Clausen, S. Hansen, and J.C. Refsgaard. 2004. Modelling of macropore flow and transport processes at catchment scale. J. Hydrol. 299:136–158. doi:10.1016/j.jhydrol.2004.04.029

Clark, M.P., D. Kavetski, and F. Fenicia. 2011. Pursuing the method of multiple working hypotheses for hydrological modeling. Water Resour. Res. 47:W09301. doi:10.1029/2010WR009827

De Schepper, G., R. Therrien, J.C. Refsgaard, and A.L. Hansen. 2015. Simulating coupled surface and subsurface water flow in a tile-drained agricultural catchment. J. Hydrol. 521:374–388. doi:10.1016/j.jhydrol.2014.12.035

Fenicia, F., D. Kavetski, H.H.G. Savenije, M.P. Clark, G. Schoups, L. Pfister, and J. Freer. 2014. Catchment properties, function, and conceptual model representation: Is there a correspondence? Hydrol. Processes 28:2451–2467. doi:10.1002/hyp.9726

Frey, S.K., H.T. Hwang, Y.J. Park, S.I. Hussain, N. Gottschall, M. Edwards, and D.R. Lapen. 2016. Dual permeability modeling of tile drain management influences on hydrologic and nutrient transport characteristics in macroporous soil. J. Hydrol. 535:392–406. doi:10.1016/j.jhydrol.2016.01.073

Gelhar, L.W., C. Welty, and K.R. Rehfeldt. 1992. A critical review of data on field-scale dispersion in aquifers. Water Resour. Res. 28:1955–1974. doi:10.1029/92WR00607

Glaser, B., J. Klaus, S. Frei, J. Frentress, L. Pfister, and L. Hopp. 2016. On the value of surface saturated area dynamics mapped with thermal infrared imagery for modeling the hillslope–riparian–stream continuum. Water Resour. Res. 52:8317–8342. doi:10.1002/2015WR018414

Graham, C.B., and H.S. Lin. 2011. Controls and frequency of preferential flow occurrence: A 175-event analysis. Vadose Zone J. 10:816–831. doi:10.2136/vzj2010.0119

Jackisch, C., L. Angermann, N. Allroggen, M. Sprenger, T. Blume, J. Tronicke, and E. Zehe. 2017. Form and function in hillslope hydrology: In situ imaging and characterization of flow-relevant structures. Hydrol. Earth Syst. Sci. 21:3749–3775. doi:10.5194/hess-21-3749-2017

Jackisch, C., and E. Zehe. 2018. Ecohydrological particle model based on representative domains. Hydrol. Earth Syst. Sci. 22:3639–3662. doi:10.5194/hess-22-3639-2018

Jansson, C., B. Espeby, and P.-E. Jansson. 2005. Preferential water flow in a glacial till soil. Nord. Hydrol. 36:1–11. doi:10.2166/nh.2005.0001

Jarvis, N., J. Koestel, and M. Larsbo. 2016. Understanding preferential flow in the vadose zone: Recent advances and future prospects. Vadose Zone J. 15(12). doi:10.2136/vzj2016.09.0075

Jarvis, N., M. Larsbo, S. Roulier, A. Lindahl, and L. Persson. 2007. The role of soil properties in regulating non-equilibrium macropore flow and solute transport in agricultural topsoils. Eur. J. Soil Sci. 58:282–292. doi:10.1111/j.1365-2389.2006.00837.x

Juilleret, J., J.F. Iffly, L. Pfister, and C. Hissler. 2011. Remarkable Pleistocene periglacial slope deposits in Luxembourg (Oesling): Pedological implication and geosite potential. Bull. Soc. Nat. Luxemb. 112(1):125–130. http://www.snl.lu/publications/bulletin/SNL_2011_112_125_130.pdf.

Klaus, J., and C.R. Jackson. 2018. Interflow is not binary: A continuous shallow perched layer does not imply continuous connectivity. Water Resour. Res. 54:5921–5932. doi:10.1029/2018WR022920

Klaus, J., C.E. Wetzel, N. Martínez-Carreras, L. Ector, and L. Pfister. 2015. A tracer to bridge the scales: On the value of diatoms for tracing fast flow path connectivity from headwaters to meso-scale catchments. Hydrol. Processes 29:5275–5289. doi:10.1002/hyp.10628

Klaus, J., and E. Zehe. 2010. Modelling rapid flow response of a tile-drained field site using a 2D physically based model: Assessment of "equifinal" model setups. Hydrol. Processes 24:1595–1609. doi:10.1002/hyp.7687

Klaus, J., and E. Zehe. 2011. A novel explicit approach to model bromide and pesticide transport in connected soil structures. Hydrol. Earth Syst. Sci. 15:2127–2144. doi:10.5194/hess-15-2127-2011

Klaus, J., E. Zehe, M. Elsner, C. Külls, and J.J. McDonnell. 2013. Macropore flow of old water revisited: Experimental insights from a tile-drained hillslope. Hydrol. Earth Syst. Sci. 17:103–118. doi:10.5194/hess-17-103-2013

Klaus, J., E. Zehe, M. Elsner, J. Palm, D. Schneider, B. Schröder, et al. 2014. Controls of event-based pesticide leaching in natural soils: A systematic study based on replicated field scale irrigation experiments. J. Hydrol. 512:528–539. doi:10.1016/j.jhydrol.2014.03.020

Köhne, J.M., S. Köhne, and H.H. Gerke. 2002. Estimating the hydraulic functions of dual-permeability models from bulk soil data. Water Resour. Res. 38(7). doi:10.1029/2001WR000492

Kordilla, J., M. Sauter, T. Reimann, and T. Geyer. 2012. Simulation of saturated and unsaturated flow in karst systems at catchment scale using a double continuum approach. Hydrol. Earth Syst. Sci. 16:3909–3923. doi:10.5194/hess-16-3909-2012

Krzeminska, D.M., T.A. Bogaard, J.-P. Malet, and L.P.H. van Beek. 2013. A model of hydrological and mechanical feedbacks of preferential fissure flow in a slow-moving landslide. Hydrol. Earth Syst. Sci. 17:947–959. doi:10.5194/hess-17-947-2013

Kukemilks, K., J.-F. Wagner, T. Saks, and P. Brunner. 2018a. Conceptualization of preferential flow for hillslope stability assessment. Hydrogeol. J. 26:439–450. doi:10.1007/s10040-017-1667-0

Kukemilks, K., J.-F. Wagner, T. Saks, and P. Brunner. 2018b. Physically based hydrogeological and slope stability modeling of the Turaida castle mound. Landslides 15:2267–2278. doi:10.1007/s10346-018-1038-5

Laine-Kaulio, H., S. Backnäs, T. Karvonen, H. Koivusalo, and J.J. McDonnell. 2014. Lateral subsurface stormflow and solute transport in a forested hillslope: A combined measurement and modeling approach. Water Resour. Res. 50:8159–8178. doi:10.1002/2014WR015381

Larsbo, M., and N. Jarvis. 2005. Simulating solute transport in a structured field soil: Uncertainty in parameter identification and predictions. J. Environ. Qual. 34:621–634. doi:10.2134/jeq2005.0621

Larsbo, M., and N. Jarvis. 2006. Information content of measurements from tracer microlysimeter experiments designed for parameter identification in dual-permeability models. J. Hydrol. 325:273–287. doi:10.1016/j.jhydrol.2005.10.020

Leistra, M., and J.J.T.I. Boesten. 2010. Measurement and computation of movement of bromide ions and carbofuran in ridged humic-sandy soil. Arch. Environ. Contam. Toxicol. 59:39–48. doi:10.1007/s00244-009-9442-4

Liu, H., and H. Lin. 2015. Frequency and control of subsurface preferential flow: From pedon to catchment scales. Soil Sci. Soc. Am. J. 79:362–377. doi:10.2136/sssaj2014.08.0330

Loritz, R., S.K. Hassler, C. Jackisch, N. Allroggen, L. van Schaik, J. Wienhöfer, and E. Zehe. 2017. Picturing and modeling catchments by representative hillslopes. Hydrol. Earth Syst. Sci. 21:1225–1249. doi:10.5194/hess-21-1225-2017

Martínez-Carreras, N., C. Hissler, L. Gourdol, J. Klaus, J. Juilleret, J.F. Iffly, and L. Pfister. 2016. Storage controls on the generation of double peak hydrographs in a forested headwater catchment. J. Hydrol. 543:255–269. doi:10.1016/j.jhydrol.2016.10.004

McGrath, G.S., C. Hinz, and M. Sivapalan. 2009. A preferential flow leaching index. Water Resour. Res. 45:W11405. doi:10.1029/2008WR007265

McGrath, G., C. Hinz, and M. Sivapalan. 2010. Assessing the impact of regional rainfall variability on rapid pesticide leaching potential. J. Contam. Hydrol. 113:56–65. doi:10.1016/j.jconhyd.2009.12.007

Meyerhoff, S.B., and R.M. Maxwell. 2011. Quantifying the effects of subsurface heterogeneity on hillslope runoff using a stochastic approach. Hydrogeol. J. 19:1515–1530. doi:10.1007/s10040-011-0753-y

Moragues-Quiroga, C., J. Juilleret, L. Gourdol, E. Pelt, T. Perrone, A. Aubert, et al. 2017. Genesis and evolution of regoliths: Evidence from trace and major elements and Sr–Nd–Pb–U isotopes. Catena 149:185–198. doi:10.1016/j.catena.2016.09.015

Reck, A., C. Jackisch, T.L. Hohenbrink, A. Zangerlé, and L. van Schaik. 2018. Impact of temporal macropore dynamics on infiltration: Field experiments and model simulations. Vadose Zone J. 17:170147. doi:10.2136/vzj2017.08.0147

Rosenbom, A.E., R. Therrien, J.C. Refsgaard, K.H. Jensen, V. Ernstsen, and K.E.S. Klint. 2009. Numerical analysis of water and solute transport in variably-saturated fractured clayey till. J. Contam. Hydrol. 104:137–152. doi:10.1016/j.jconhyd.2008.09.001

Roulier, S., N. Baran, C. Mouvet, F. Stenemo, X. Morvan, H.J. Albrechtsen, et al. 2006. Controls on atrazine leaching through a soil–unsaturated fractured limestone sequence at Brévilles, France. J. Contam. Hydrol. 84:81–105. doi:10.1016/j.jconhyd.2005.12.004

Scaini, A., M. Audebert, C. Hissler, F. Fenicia, L. Gourdol, L. Pfister, and K.J. Beven. 2017. Velocity and celerity dynamics at plot scale inferred from artificial tracing experiments and time-lapse ERT. J. Hydrol. 546:28–43. doi:10.1016/j.jhydrol.2016.12.035

Scaini, A., C. Hissler, F. Fenicia, J. Juilleret, J.-F. Iffly, L. Pfister, and K.J. Beven. 2018. Hillslope response to sprinkling and natural rainfall using velocity and celerity estimates in a slate-bedrock catchment. J. Hydrol. 558:366–379. doi:10.1016/j.jhydrol.2017.12.011

Scheibe, T.D., W.A. Perkins, M.C. Richmond, M.I. McKinley, P.D.J. Romero-Gomez, M. Oostrom, et al. 2015. Pore-scale and multiscale numerical simulation of flow and transport in a laboratory-scale column. Water Resour. Res. 51:1023–1035. doi:10.1002/2014WR015959

Schwab, M.P., J. Klaus, L. Pfister, and M. Weiler. 2017. How runoff components affect the export of DOC and nitrate: A long-term and high-frequency analysis. Hydrol. Earth Syst. Sci. Discuss. doi:10.5194/hess-2017-416

Steinbrich, A., H. Leistert, and M. Weiler. 2016. Model-based quantification of runoff generation processes at high spatial and temporal resolution. Environ. Earth Sci. 75:1423. doi:10.1007/s12665-016-6234-9

Therrien, R., R.G. McLaren, E.A. Sudicky, and S.M. Panday. 2010. HydroGeoSphere: A three-dimensional numerical model describing fully-integrated subsurface and surface flow and solute transport. Groundwater Simulations Group, Univ. of Waterloo, Waterloo, ON, Canada.

van Schaik, N.L.M.B., A. Bronstert, S.M. De Jong, V.G. Jetten, J.C. Van Dam, C.J. Ritsema, and S. Schnabel. 2014. Process-based modelling of a headwater catchment in a semi-arid area : The influence of macropore flow. Hydrol. Processes 28:5805–5816. doi:10.1002/hyp.10086

van Schaik, N.L.M.B., R.F.A. Hendriks, and J.C. van Dam. 2010. Parameterization of macropore flow using dye-tracer infiltration patterns in the SWAP model. Vadose Zone J. 9:95–106. doi:10.2136/vzj2009.0031

Villamizar, M.L., and C.D. Brown. 2017. A modelling framework to simulate river flow and pesticide loss via preferential flow at the catchment scale. Catena 149:120–130. doi:10.1016/j.catena.2016.09.009

Vogel, H.-J., I. Cousin, O. Ippisch, and P. Bastian. 2006. The dominant role of structure for solute transport in soil: Experimental evidence and modelling of structure and transport in a field experiment. Hydrol. Earth Syst. Sci. 10:495–506. doi:10.5194/hess-10-495-2006

Vogel, H., and K. Roth. 2003. Moving through scales of flow and transport in soil. J. Hydrol. 272:95–106. doi:10.1016/S0022-1694(02)00257-3

Wang, Y., S.A. Bradford, and J. Šimůnek. 2014. Estimation and upscaling of dual-permeability model parameters for the transport of E. coli D21g in soils with preferential flow. J. Contam. Hydrol. 159:57–66. doi:10.1016/j.jconhyd.2014.01.009

Weiler, M. 2017. Macropores and preferential flow: A love–hate relationship. Hydrol. Processes 31:15–19. doi:10.1002/hyp.11074

Weiler, M., and J.J. McDonnell. 2007. Conceptualizing lateral preferential flow and flow networks and simulating the effects on gauged and ungauged hillslopes. Water Resour. Res. 43:W03403. doi:10.1029/2006WR004867

Wiekenkamp, I., J.A. Huisman, H.R. Bogena, H.S. Lin, and H. Vereecken. 2016. Spatial and temporal occurrence of preferential flow in a forested headwater catchment. J. Hydrol. 534:139–149. doi:10.1016/j.jhydrol.2015.12.050

Wilson, G.V., J.R. Rigby, M. Ursic, and S.M. Dabney. 2016. Soil pipe flow tracer experiments: 1. Connectivity and transport characteristics. Hydrol. Processes 30:1265–1279. doi:10.1002/hyp.10713

Wrede, S., F. Fenicia, N. Martínez-Carreras, J. Juilleret, C. Hissler, A. Krein, et al. 2015. Towards more systematic perceptual model development: A case study using 3 Luxembourgish catchments. Hydrol. Processes 29:2731–2750. doi:10.1002/hyp.10393

Yu, X., C. Duffy, D.C. Baldwin, and H. Lin. 2014. The role of macropores and multi-resolution soil survey datasets for distributed surface–subsurface flow modeling. J. Hydrol. 516:97–106. doi:10.1016/j.jhydrol.2014.02.055

Zehe, E., and G. Blöschl. 2004. Predictability of hydrologic response at the plot and catchment scales: Role of initial conditions. Water Resour. Res. 40:W10202. doi:10.1029/2003WR002869

Zhang, G.P., H.H.G. Savenije, F. Fenicia, and L. Pfister. 2006. Modelling subsurface storm flow with the representative elementary watershed (REW) approach: Application to the Alzette River basin. Hydrol. Earth Syst. Sci. 10:937–955. doi:10.5194/hess-10-937-2006